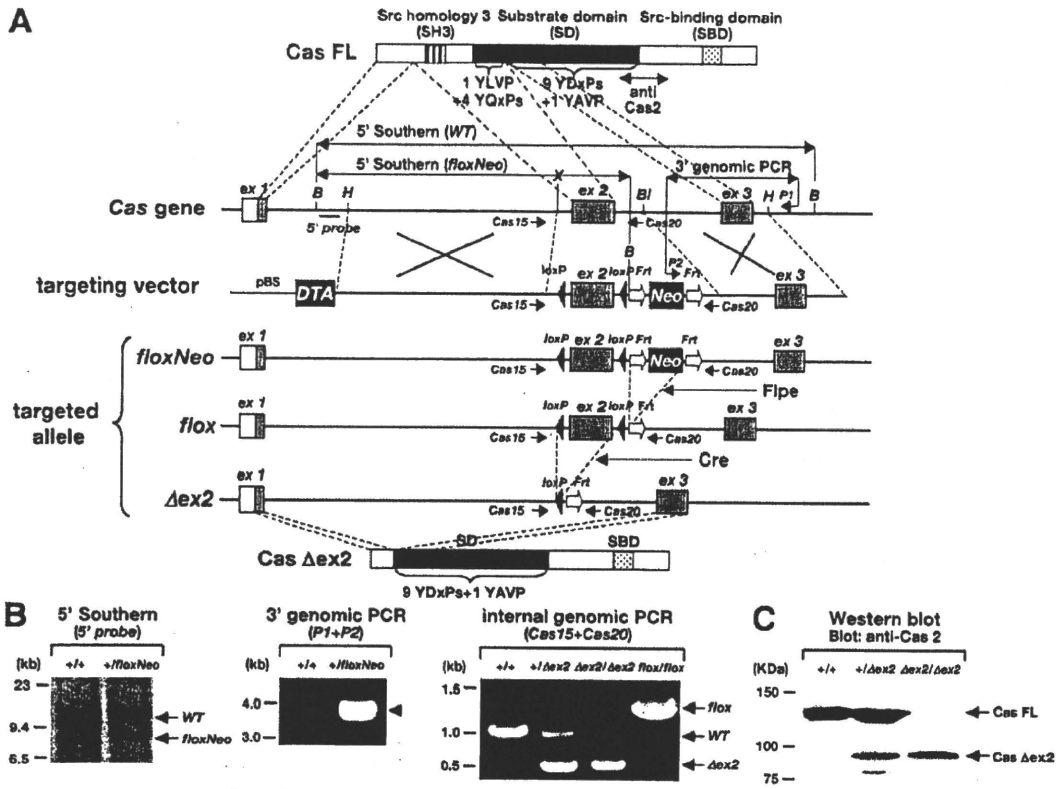

Fig. 1. Generation of Cas exon 2-specific knockout mice. (A) Schematic structure of the Cas FL protein, the knockout procedure, and the resulting Cas Δex2 protein. The region containing Cas exon 2, which encodes the entire SH3 domain and part of the SD containing one YLVP motif and four YQXP motifs, was replaced with a targeting vector in which exon 2 was flanked by two *loxP* sites followed by *Neo*. The neomycin cassette was removed by Flpe recombinase, and Cas exon 2 was removed by Cre recombinase. Expected lengths of *Bam*HI-digested 5′ Southern and 3′ genomic PCR fragments are shown, and the positions of PCR primers used for genotyping (*P1*, *P2*, *Cas15*, and *Cas20*) are indicated. The restriction enzymes were *Bam*HI (*B*), *Hind*III (*H*), *Xba*I (*X*), and *Bln*I (*Bl*). (B) Genotyping of embryonic stem cells and mice. Correctly targeted embryonic stem cells were identified by 5′ Southern blotting and 3′ genomic PCR. Flpe-mediated *Neo* deletion and Cre-mediated exon 2 deletion in mice were confirmed by internal genomic PCR. Molecular markers are shown on the left. (C) Western blot analysis showing the generation of the Cas Δex2 protein in $Cas^{\Delta ex2/\Delta ex2}$ mice. Western blotting with anti-Cas2 detected the expected size of the Cas Δ exon 2 protein[32] in $Cas^{\Delta ex2/\Delta ex2}$ mice. Molecular markers are shown on the left.

found in other organs, including the brain, heart, lungs, spleen, and kidneys (data not shown). Therefore, we concluded that progressive liver degeneration was the primary cause of death of $Cas^{\Delta ex2/\Delta ex2}$ embryos. The pathological pictures suggested that the progressive hepatocyte reduction in $Cas^{\Delta ex2/\Delta ex2}$ embryos was due to apoptosis. To address this possibility, livers of $Cas^{\Delta ex2/\Delta ex2}$ and WT embryos 12.5 dpc were subjected to the TUNEL assay. As shown in Fig. 2C, no obvious staining was observed in the WT liver (left panels), whereas several round hepatocytes surrounding the central collapsed area were positively stained in the $Cas^{\Delta ex2/\Delta ex2}$ liver (indicated by arrowheads in the right bottom panel); this confirmed the apoptotic reduction of hepatocytes.

Cas Was Preferentially Expressed in SECs in the Developing Liver. To investigate the mechanism underlying hepatocyte apoptosis, localization of the Cas protein in the embryonic liver was examined by immunohistochemistry. Normal livers at 11.5 dpc, when liver degeneration began to occur in $Cas^{\Delta ex2/\Delta ex2}$ embryos (see Fig. 2A,B), were stained with an anti-Cas

Table 1. Survival of Offspring Obtained by the Crossing of $Cas^{+/\Delta ex2}$ Mice

Stage	Total Litter Number	Genotype		
		+/+	+/Δex2	Δex2/Δex2 (dead)
11.5 dpc	15	2	11	2
12.5 dpc	52	16	22	14
13.5 dpc	22	7	10	5 (5)
14.5 dpc	14	4	8	2 (2)
15.5 dpc	10	4	4	2 (2)
16.5 dpc	4	1	3	0
Postnatal	49	15	34	0

Genotyping was performed by PCR analysis of tail DNA. Embryo survival was defined as a beating heart.

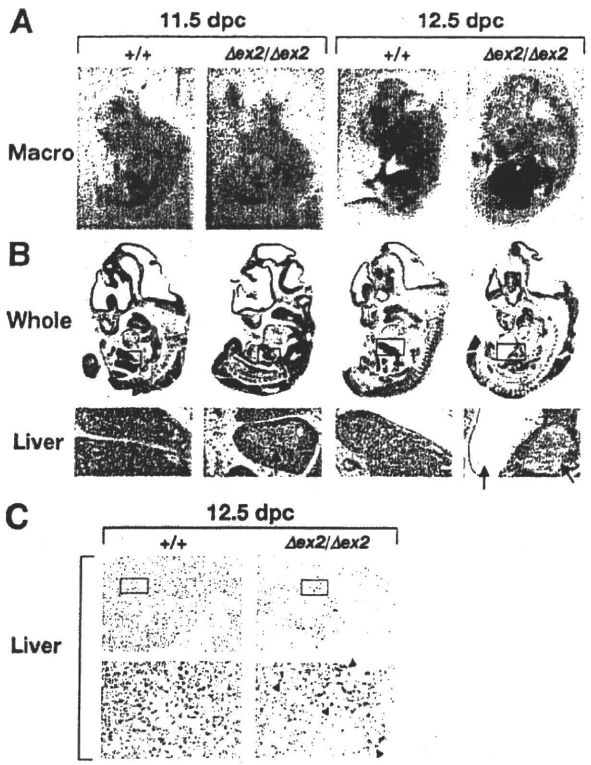

Fig. 2. Histological analysis and TUNEL staining of $Cas^{+/+}$ and $Cas^{\Delta ex2/\Delta ex2}$ embryos. (A) Macroscopic appearance of $Cas^{+/+}$ and $Cas^{\Delta ex2/\Delta ex2}$ embryos at 11.5 and 12.5 dpc. The enlarged liver capsule and internal hematoma in $Cas^{\Delta ex2/\Delta ex2}$ mice at 12.5 dpc are indicated by black and white triangles, respectively. (B) HE-stained sagittal sections of $Cas^{+/+}$ and $Cas^{\Delta ex2/\Delta ex2}$ embryos at 11.5 and 12.5 dpc. The livers in the whole sections are boxed, and they are magnified in the lower sections. Note the progressive reduction of parenchymal hepatocytes and cavity and hematoma formation in the $Cas^{\Delta ex2/\Delta ex2}$ liver (indicated by arrows). (C) TUNEL assay of $Cas^{+/+}$ and $Cas^{\Delta ex2/\Delta ex2}$ livers at 12.5 dpc. The boxed areas in the upper sections are magnified in the lower sections. Apoptotic cells, identified by brown staining, were detected in the $Cas^{\Delta ex2/\Delta ex2}$ liver (indicated by arrowheads).

antibody. In agreement with our previous report,[22] Cas expression was barely detectable in parenchymal hepatocytes but was readily detected in cells lining microvessels, which morphologically resembled SECs (indicated by arrowheads in the right panel of Fig. 3A). To confirm that Cas is mainly expressed in nonparenchymal cells, liver cells were separated into parenchymal and nonparenchymal fractions and subjected to anti-Cas staining. As shown in the upper panels of Fig. 3B, the parenchymal fraction contained hepatocyte-like cells, whereas the nonparenchymal fraction contained stroma-like cells; this indicated that the separation was successfully performed. Anti-Cas staining showed that no positive staining was observed in cells of the parenchymal fraction (lower left panel of Fig. 3B), whereas some cells in the nonparenchymal fraction gave positive signals (indicated by arrows in the lower right panel of Fig. 3B); this indicated that Cas expression was confined to nonparenchymal cells. To directly examine whether Cas is expressed in SECs, liver sections were immunofluorescently stained with an anti-Cas antibody and an anti–stabilin 2 (anti-Stab2) antibody that specifically detects SECs.[29] As shown in Fig. 3C, anti-Cas staining (top panel, shown in green) and anti-Stab2 staining (second panel, shown in red) largely overlapped (third panel, shown in yellow and indicated by arrows); this demonstrated that Cas is preferentially expressed in SECs. We further examined whether Cas expression is developmentally associated with the maturation of liver sinusoids. Previous reports have demonstrated that liver bud formation begins at 9.5 dpc[30] and that the basic structure of hepatic sinusoids becomes established at 12.5 dpc.[31] Thus, livers of embryos 9.5 to 12.5 dpc were stained with an anti-Cas antibody. As shown in Supporting Fig. 1, Cas immunoreactivity appeared detectable around the sinusoids at 10.5 dpc and became enhanced at 11.5 and 12.5 dpc. These results indicate that Cas is preferentially expressed in SECs during liver development and strongly suggest that the apoptotic hepatocyte reduction in $Cas^{\Delta ex2/\Delta ex2}$ embryos is ascribable not to cell-intrinsic defects but rather to dysfunction of SECs.

Expression of Cas Devoid of the SH3 Domain (Cas ΔSH3) in SECs Markedly Attenuates Cas Tyrosine Phosphorylation and Reduces Cas-CrkII Association. Because the primary culture of SECs from $Cas^{\Delta ex2/\Delta ex2}$ embryos was not expected to be feasible, we established an *in vitro* system using a rat SEC line (NP31).[25] NP31 cells retain functional features for SECs, such as uptake of acetylated low-density lipoprotein and tubular network formation,[25] and also preserve morphological characteristics for SECs (the transcellular pores called fenestrae[1,3]; shown later in Fig. 5B). Because NP31 cells express endogenous Cas (Fig. 4B, right panel), to generate NP31 cells mimicking $Cas^{\Delta ex2/\Delta ex2}$ SECs, we overexpressed Cas devoid of the SH3 domain (Cas ΔSH3), the main functional module of exon 2, in NP31 cells. To confirm that the phenotypes of Cas ΔSH3–overexpressing NP31 cells were due to SH3 deletion and not to overexpression of other functional domains, we also established NP31 cells overexpressing Cas FL. HA-tagged Cas FL and Cas ΔSH3 (Fig. 4A)[28] were retrovirally introduced into NP31 cells, and the expression levels of their protein products were examined by western blotting with an anti-HA antibody that detects exogenous Cas and

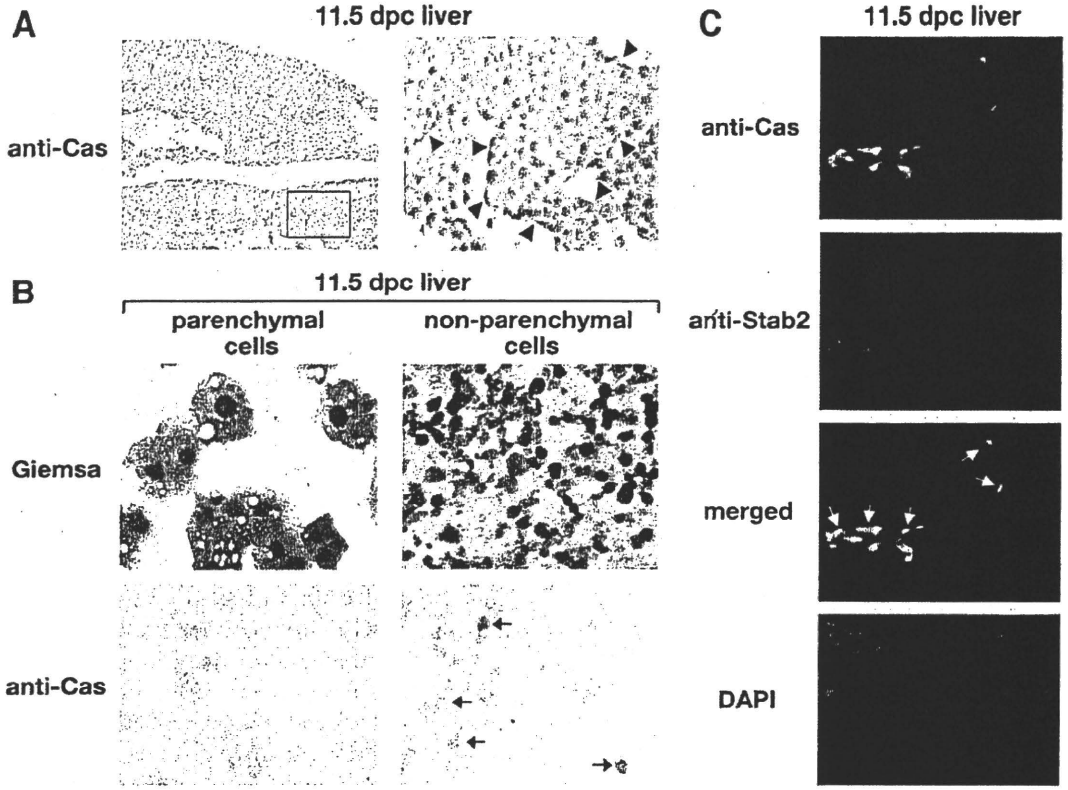

Fig. 3. Cas expression in SECs in the embryonic liver. (A) Localization of Cas in the embryonic liver. The $Cas^{+/+}$ liver at 11.5 dpc was immunohistochemically stained with an anti-Cas antibody. The boxed area in the left panel is magnified in the right panel. Positive signals were not present in hepatocytes but were present in cells around the sinusoids (indicated by arrowheads). (B) Cas expression in hepatic parenchymal and nonparenchymal cells. Hepatic cells of the $Cas^{-/-}$ liver at 11.5 dpc were separated into parenchymal and nonparenchymal fractions and stained with an anti-Cas antibody. The Giemsa-stained morphological appearance and anti-Cas staining patterns of the cells are shown in the upper and lower panels, respectively. Positively stained cells in the nonparenchymal fraction are indicated by arrows. (C) Cas expression in SECs. The $Cas^{+/+}$ liver at 11.5 dpc was immunofluorescently stained with an anti-Cas antibody (green) and with anti-Stab2, an anti-SEC antibody (red). Anti-Cas and anti-Stab2 immunoreactivities were merged, and overlapped areas (yellow) are indicated by arrows. DAPI staining is shown to identify nuclei of the cells.

also with an anti-Cas antibody that detects endogenous and exogenous Cas. As shown in Fig. 4B, Cas FL and Cas ΔSH3 were expressed at almost comparable levels (left panel) that were approximately 5 to 6 times greater than those of endogenous Cas (right panel). To examine the effect of SH3 deletion on Cas-mediated signaling, cells were plated onto fibronectin (FN)-coated dishes, and the cell lysates were subjected to immunoprecipitation followed by western blotting. As shown in Fig. 4C, anti-HA and anti-Cas2 immunoprecipitates blotted by an anti-phosphotyrosine antibody (4G10) showed that Cas ΔSH3 was much less tyrosine-phosphorylated than Cas FL (left panel), and tyrosine phosphorylation of endogenous Cas was barely detectable in Cas ΔSH3–expressing cells (right panel). In addition, as shown in Fig. 4D, anti-CrkII immunoprecipitates blotted by anti-HA or anti-Cas2 antibodies revealed that Cas ΔSH3 was far less efficiently coprecipitated with CrkII than Cas FL (left panel), and CrkII did not detectably coprecipitate endogenous Cas in lysates from Cas ΔSH3–expressing cells (right panel). These findings indicate that Cas ΔSH3 functions as a reduction-of-function molecule in NP31 cells as $Cas^{\Delta ex2/\Delta ex2}$ does in mouse embryonic fibroblasts (MEFs).[32]

Impaired Actin Stress Fiber Formation and Loss of Fenestrae in NP31 Cells Expressing Cas ΔSH3. To examine the suppressive function of Cas ΔSH3 on actin stress fiber formation, parental, Cas FL–expressing, and Cas ΔSH3–expressing NP31 cells were subjected to cytoskeletal staining. As shown in Fig. 5A, prominent actin stress fiber formation was detected in parental cells and to a comparable extent in Cas FL–expressing cells (indicated by arrows in the lower left and middle panels). In contrast, no obvious actin stress fibers were formed and only dotlike actin filaments were observed in Cas ΔSH3–expressing NP31 cells (indicated by arrowheads in the lower right

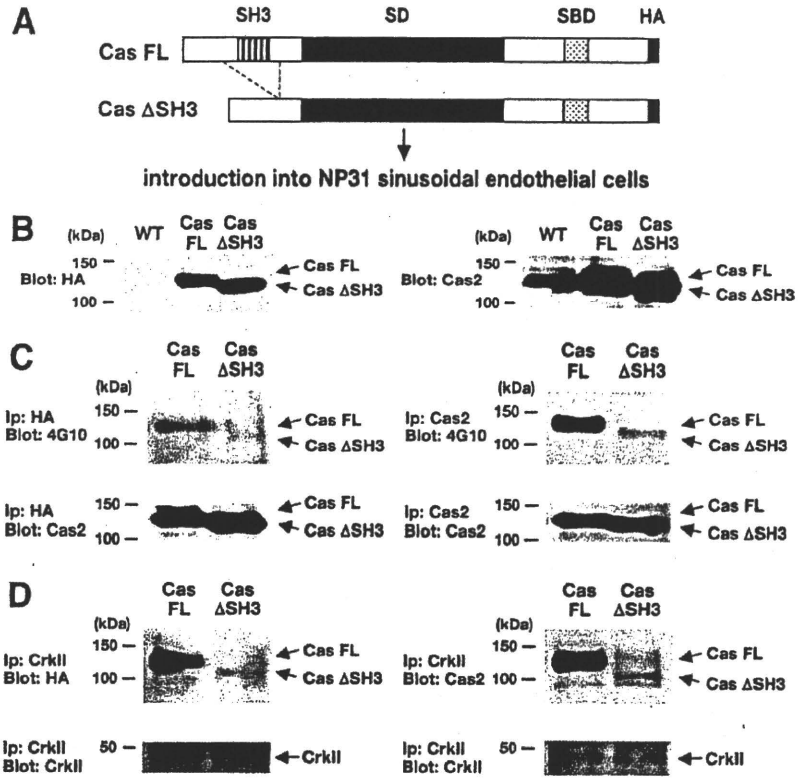

Fig. 4. Expression, tyrosine phosphorylation, and binding ability of Cas FL and Cas ΔSH3 to CrkII in NP31 SECs. (A) Schematic structure of Cas constructs used in the assay. HA-tagged Cas FL and Cas ΔSH3 cDNAs were retrovirally introduced into NP31 SECs. (B) Expression levels of Cas FL and Cas ΔSH3 in NP31 cells. Proteins extracted from WT, Cas FL-expressing, and Cas ΔSH3-expressing NP31 cells were blotted with anti-HA (left) or anti-Cas2 antibodies (right). The positions of Cas FL and Cas ΔSH3 are indicated, and molecular markers are shown on the left. (C) Tyrosine phosphorylation of Cas FL and Cas ΔSH3 in NP31 cells. Proteins extracted from Cas FL-expressing and Cas ΔSH3-expressing NP31 cells plated on FN were immunoprecipitated with anti-HA (left) or anti-Cas2 antibodies (right), and immunoprecipitated proteins were blotted with an anti-phosphotyrosine antibody, 4G10 (top), or an anti-Cas2 antibody (bottom). The positions of Cas FL and Cas ΔSH3 are indicated, and molecular markers are shown on the left. (D) Binding ability of Cas FL and Cas ΔSH3 in NP31 cells. Proteins extracted from Cas FL-expressing and Cas ΔSH3-expressing NP31 cells plated on FN were immunoprecipitated with an anti-CrkII antibody, and immunoprecipitated proteins were blotted with anti-HA (left top), anti-Cas2 (right top), or anti-CrkII antibodies (bottom). The positions of Cas FL and Cas ΔSH3 are indicated, and molecular markers are shown on the left.

panel). We then investigated the formation of fenestrae in NP31 cells by electron microscopy because the architectural control of fenestrae is regulated by the actin cytoskeleton.[1,3,7] Parental and Cas FL–expressing NP31 cells exhibited a number of fenestrae of various diameters (left and middle panels in Fig. 5B). Counting of the fenestrae per square micrometer showed that although the number of fenestrae in Cas FL–expressing cells was slightly higher than that in parental cells (5.80 ± 0.37 for parental cells and 6.13 ± 0.39 for Cas FL–expressing NP31 cells), the difference was not statistically significant (left and middle bars in Fig. 5C). Remarkably, the formation of fenestrae was almost completely abolished in Cas ΔSH3–expressing cells, and few small, fenestra-like pores were observed (indicated by arrowheads in the right lower panel of Fig. 5B). The number of fenestrae in Cas ΔSH3–expressing cells was 0.58 ± 0.16, which was statistically significantly low in comparison with those in parental and Cas FL–expressing NP31 cells ($P < 0.001$; left right bars and middle right bars in Fig. 5C). These results strongly indicate that Cas plays pivotal roles in the regulation of the actin cytoskeleton and in the formation of fenestrae in SECs.

Discussion

Cas is an adaptor/scaffold protein that contributes to various biological processes through the regulation of actin stress fiber formation.[9,10] Upon physiological and pathological stimuli, Cas becomes tyrosine-phosphorylated mainly in the SD, which offers binding sites for the SH2 domain of downstream target molecules, including CrkII.[9,10] The Cas/CrkII complex

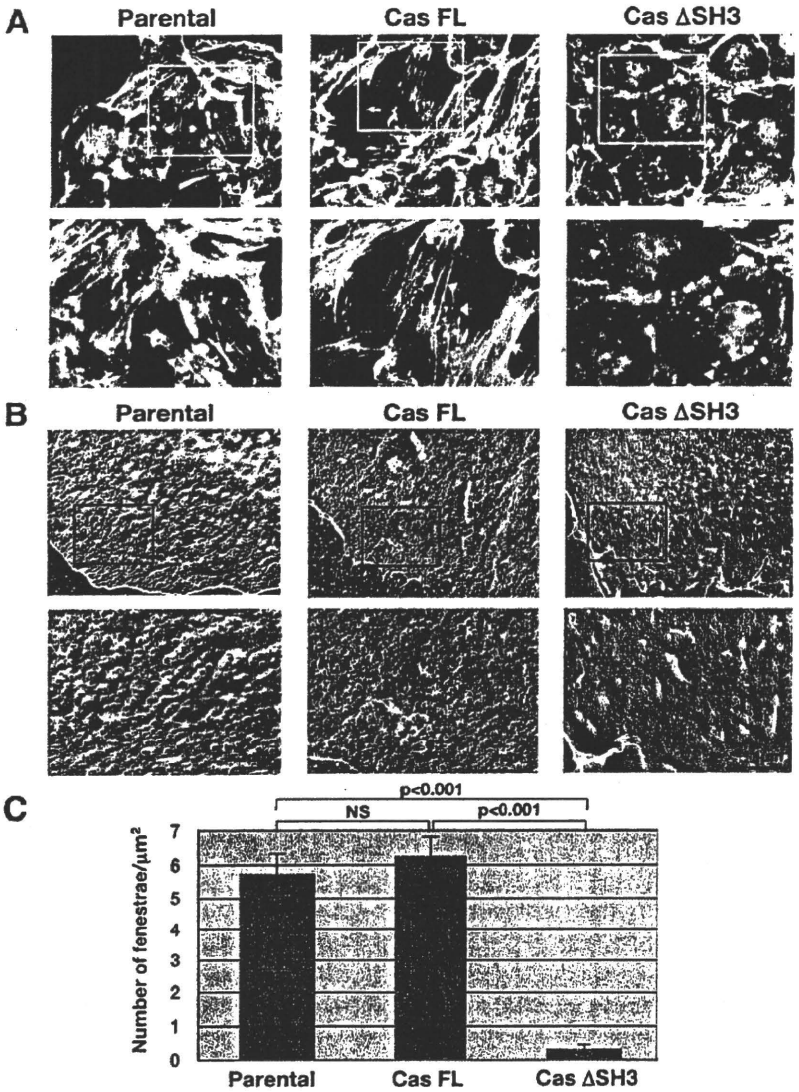

Fig. 5. Actin stress fiber formation and fenestra formation in parental, Cas FL–expressing, and Cas ΔSH3-expressing NP31 cells. (A) Actin stress fiber formation. Parental, Cas FL–expressing, and Cas ΔSH3-expressing NP31 cells were stained with phalloidin. The boxed areas in the upper panels are magnified in the lower panels. Thick, dense, and long actin fibers in parental and Cas FL-expressing NP31 cells and dotlike actin filaments in Cas ΔSH3-expressing NP31 cells are indicated by arrows and arrowheads, respectively. (B) Fenestra formation. Parental, Cas FL–expressing, and Cas ΔSH3-expressing NP31 cells were analyzed under an electron microscope. The boxed areas in the upper panels are magnified in the lower panels. Although a number of fenestrae were found in parental and Cas FL-expressing NP31 cells, only a few porelike regions were detected in Cas ΔSH3-expressing NP31 cells (arrowheads). (C) Number of fenestrae per square micrometer. Data are plotted as means and error bars. The number of fenestrae was significantly reduced in Cas ΔSH3-expressing NP31 cells versus parental and Cas FL-expressing NP31 cells ($P < 0.001$). Abbreviation: NS, not significant.

sequentially activates downstream effectors, such as Rac and C3G, which consequently reorganize the actin cytoskeleton and finally define cellular dynamics.[9,10]

We previously generated mice lacking Cas ($Cas^{-/-}$) and demonstrated that they died *in utero* and exhibited cardiovascular anomalies.[22] In the present study, we generated mice carrying a hypomorphic Cas allele lacking the exon 2–derived region. Exon 2 was targeted in this study for several reasons. First, it is the only exon that encodes the whole region of a functional domain of Cas.[8] Second, it encodes SH3, which binds to the proline-rich region of focal adhesion kinase[11] and mediates the initial signaling event from the extracellular matrix to intracellular molecules.[32,33] Third, our previous compensation study revealed the importance of SD and SB for cell migration and cell transformation, respectively, but the role of SH3 is less understood.[28]

Mice harboring Cas with an exon 2 deletion ($Cas^{\Delta ex2/\Delta ex2}$) died as embryos (Table 1) but differed in phenotype from $Cas^{-/-}$ mice; $Cas^{\Delta ex2/\Delta ex2}$ mice exhibited impaired liver development with massive hepatocyte apoptosis (Fig. 2), and in contrast to $Cas^{-/-}$ mice, their cardiovascular system was preserved, presumably because of the conserved ability of Cas Δex2 to partially become tyrosine-phosphorylated and retain CrkII binding[32] (Fig. 4). In the former work,[22] we noted that $Cas^{-/-}$ mice also showed retarded liver growth. We previously hypothesized it to be secondary to circulatory failure because the Cas protein was barely detectable in hepatocytes, as in this study[22] (Fig. 3). However, the current observation that

$Cas^{\Delta ex2/\Delta ex2}$ mice exhibit liver degeneration without suffering from cardiovascular anomalies strongly implies that dysfunction of Cas directly impairs liver development.

The findings that Cas is preferentially expressed in SECs in the liver (Fig. 3) and that the expression patterns of Cas well correlate with the maturation of sinusoids (Supporting Fig. 1) indicate that Cas is functionally and developmentally involved in SECs and strongly suggest that Cas Δex2 impairs SEC function and leads to hepatocyte apoptosis. To confirm this, we employed an SEC line, NP31, as a model system and investigated the effect of Cas Δex2 on SEC function. Our previous study using MEFs derived from $Cas^{\Delta ex2/\Delta ex2}$ mice showed that Cas Δex2 possesses reduced function in FN-mediated signaling.[32] Thus, to examine the Cas requirement for SEC function, we first attempted to knock down endogenous Cas in NP31 cells by RNA interference. However, we found that NP31 cells rapidly lost fenestra formation when they were exposed to transfection reagents with nonspecific small interfering RNA or even no RNA (data not shown). We thus used an alternative Cas mutant overexpression approach. We used Cas ΔSH3 because the SH3 domain represents virtually the functional domain of exon 2 (Fig. 1) and other motifs in exon 2, YLVP and YQxPs, have been demonstrated to be redundant or dispensable for Cas-mediated signaling.[34] In fact, Cas ΔSH3–expressing NP31 cells exhibited biochemical properties similar to those of $Cas^{\Delta ex2/\Delta ex2}$ MEFs, such as impaired Cas tyrosine phosphorylation and reduced interaction of Cas with CrkII[32] (Fig. 4). Thus, Cas ΔSH3 is biochemically equivalent to and functionally recapitulates Cas exon 2 deletion. In agreement with these biochemical alterations, we demonstrated that Cas ΔSH3 abolished reorganization of the actin cytoskeleton and critically inhibited the formation of fenestrae (Fig. 5). These findings strongly indicate that the Cas exon 2 deficiency affected actin cytoskeleton reorganization and SEC fenestration in $Cas^{\Delta ex2/\Delta ex2}$ embryos, and the impaired SEC fenestration subsequently induced massive hepatocyte apoptosis during liver development. Previous *in vitro* studies in SECs showed that treatment of the cells with anti-actin agents and artificial modulation of Rho small GTPases impaired SEC fenestration[35-40]; in addition, SEC fenestration was required for hepatocyte survival.[5,6] These findings are consistent with the notion described previously.

The current study highlights the importance of Cas in liver development. It also unveils an unexpectedly intimate interaction between SEC cytoskeletal turnover and hepatocyte development by illustrating the indirect influence of SEC fenestration on hepatocyte survival. It has previously been reported that the numbers and diameters of fenestrae are sensitive to growth factors such as vascular endothelial growth factor,[41-43] endothelin-1,[44-46] and transforming growth factor β.[43] Intriguingly, these factors are known to tyrosine-phosphorylate Cas,[47-49] and this strongly suggests that Cas tyrosine phosphorylation is involved in the induced changes of fenestrae. Defenestration has been reported in various liver diseases such as alcoholic liver damage,[50,51] hepatitis and liver cirrhosis,[52,53] and liver cancer[54,55] and causes portal hypertension and liver dysfunction.[1] A recent report demonstrated that the administration of a vascular endothelial growth factor–expressing plasmid through the portal vein in cirrhotic rats resulted in increased numbers of fenestrae and decreased portal vein pressure.[56] Collectively, these findings, including ours, suggest a potential therapeutic approach that regulates SEC fenestration, and they raise Cas as a novel molecular target in protective and regenerative therapy for SEC-defenestrating liver diseases.

Acknowledgment: The authors thank Kazuko Miyazaki for construction of the targeting vector and embryonic stem cell screening; Yuki Sakai, Kayoko Hashimoto, Yuko Tsukawaki, Rika Tai, and Aiko Kinomura for mouse care and technical assistance; Mitsuhiro Watanabe for help with the electron microscopy analysis; Yoshiro Maru and Masabumi Shibuya for the NP31 cells; Toshio Kitamura for the pMxIG vector and Plat-E cells; and Atsushi Miyajima for the anti-Stab2 antibody.

References

1. Braet F, Wisse E. Structural and functional aspects of liver sinusoidal endothelial cell fenestrae: a review. Comp Hepatol 2002;23:1–17.
2. Higuchi H, Gores GJ. Mechanisms of liver injury: an overview. Curr Mol Med 2003;3:483–490.
3. Braet F. How molecular microscopy revealed new insights into the dynamics of hepatic endothelial fenestrae in the past decade. Liver Int 2004;24:532–539.
4. Langer DA, Das A, Semela D, Kang-Decker N, Hendrickson H, Bronk SF, et al. Nitric oxide promotes caspase-independent hepatic stellate cell apoptosis through the generation of reactive oxygen species. HEPATOLOGY 2008;47:1983–1993.
5. Warren A, Le Couteur DG, Fraser R, Bowen DG, McCaughan GW, Bertolino P. T lymphocytes interact with hepatocytes through fenestrations in murine liver sinusoidal endothelial cells. HEPATOLOGY 2006;44:1182–1190.
6. March S, Hui EE, Underhill GH, Khetani S, Bhatia SN. Microenvironmental regulation of the sinusoidal endothelial cell phenotype *in vitro*. HEPATOLOGY 2009;50:920–928.
7. Yokomori H. New insights into the dynamics of sinusoidal endothelial fenestrae in liver sinusoidal endothelial cells. Med Mol Morphol 2008;41:1–4.

8. Sakai R, Iwamatsu A, Hirano N, Ogawa S, Tanaka T, Mano H, et al. A novel signaling molecule, p130, forms stable complexes *in vivo* with v-Crk and v-Src in a tyrosine phosphorylation-dependent manner. EMBO J 1994;13:3748–3756.
9. Bouton AH, Riggins RB, Bruce-Staskal PJ. Functions of the adapter protein Cas: signal convergence and the determination of cellular responses. Oncogene 2001;20:6448–6458.
10. Defilippi P, Di Stefano P, Cabodi S. p130Cas: a versatile scaffold in signaling networks. Trends Cell Biol 2006;16:257–263.
11. Polte TR, Hanks SK. Interaction between focal adhesion kinase and Crk-associated tyrosine kinase substrate p130Cas. Proc Natl Acad Sci U S A 1995;92:10678–10682.
12. Harte MT, Hildebrand JD, Burnham MR, Bouton AH, Parsons JT. p130Cas, a substrate associated with v-Src and v-Crk, localizes to focal adhesions and binds to focal adhesion kinase. J Biol Chem 1996;271: 13649–13655.
13. Lakkakorpi PT, Nakamura I, Nagy RM, Parsons JT, Rodan GA, Duong LT. Stable association of PYK2 and p130(Cas) in osteoclasts and their colocalization in the sealing zone. J Biol Chem 1999;274: 4900–4907.
14. Liu F, Hill DE, Chernoff J. Direct binding of the proline-rich region of protein tyrosine phosphatase 1B to the Src homology 3 domain of p130(Cas). J Biol Chem 1996;271:31290–31295.
15. Garton AJ, Burnham MR, Bouton AH, Tonks NK. Association of PTP-PEST with the SH3 domain of p130cas; a novel mechanism of protein tyrosine phosphatase substrate recognition. Oncogene 1997;15: 877–885.
16. Kirsch KH, Georgescu MM, Hanafusa H. Direct binding of p130(Cas) to the guanine nucleotide exchange factor C3G. J Biol Chem 1998; 273:25673–25679.
17. Nakamoto T, Yamagata T, Sakai R, Ogawa S, Honda H, Ueno H, et al. CIZ, a zinc finger protein that interacts with p130(cas) and activates the expression of matrix metalloproteinases. Mol Cell Biol 2000; 20:1649–1658.
18. Mayer BJ, Hirai H, Sakai R. Evidence that SH2 domains promote processive phosphorylation by protein-tyrosine kinases. Curr Biol 1995; 5:296–305.
19. Schlaepfer DD, Broome MA, Hunter T. Fibronectin-stimulated signaling from a focal adhesion kinase-c-Src complex: involvement of the Grb2, p130cas, and Nck adaptor proteins. Mol Cell Biol 1997;17: 1702–1713.
20. Prasad N, Topping RS, Decker SJ. SH2-containing inositol 5′-phosphatase SHIP2 associates with the p130(Cas) adapter protein and regulates cellular adhesion and spreading. Mol Cell Biol 2001;21: 1416–1428.
21. Nakamoto T, Sakai R, Ozawa K, Yazaki Y, Hirai H. Direct binding of C-terminal region of p130Cas to SH2 and SH3 domains of Src kinase. J Biol Chem 1996;271:8959–8965.
22. Honda H, Oda H, Nakamoto T, Honda Z, Sakai R, Suzuki T, et al. Cardiovascular anomaly, impaired actin bundling and resistance to Src-induced transformation in mice lacking p130Cas. Nat Genet 1998;19: 361–365.
23. Honda H, Nakamoto T, Sakai R, Hirai H. p130(Cas), an assembling molecule of actin filaments, promotes cell movement, cell migration, and cell spreading in fibroblasts. Biochem Biophys Res Commun 1999; 262:25–30.
24. Ishiguro S, Arii S, Monden K, Adachi Y, Funaki N, Higashitsuji H, et al. Identification of the thromboxane A2 receptor in hepatic sinusoidal endothelial cells and its role in endotoxin-induced liver injury in rats. HEPATOLOGY 1994;20:1281–1286.
25. Maru Y, Yamaguchi S, Takahashi T, Ueno H, Shibuya M. Virally activated Ras cooperates with integrin to induce tubulogenesis in sinusoidal endothelial cell lines. J Cell Physiol 1998;176:223–234.
26. Kitamura T, Koshino Y, Shibata F, Oki T, Nakajima H, Nosaka T, et al. Retrovirus-mediated gene transfer and expression cloning: powerful tools in functional genomics. Exp Hematol 2003;31: 1007–1014.
27. Morita S, Kojima T, Kitamura T. Plat-E: an efficient and stable system for transient packaging of retroviruses. Gene Ther 2000;7: 1063–1066.
28. Huang J, Hamasaki H, Nakamoto T, Honda H, Hirai H, Saito M, et al. Differential regulation of cell migration, actin stress fiber organization, and cell transformation by functional domains of Crk-associated substrate. J Biol Chem 2002;277:27265–27272.
29. Nonaka H, Tanaka M, Suzuki K, Miyajima A. Development of murine hepatic sinusoidal endothelial cells characterized by the expression of hyaluronan receptors. Dev Dyn 2007;236:2258–2267.
30. Matsumoto K, Yoshitomi H, Rossant J, Zaret KS. Liver organogenesis promoted by endothelial cells prior to vascular function. Science 2001; 294:559–563.
31. Enzan H, Himeno H, Hiroi M, Kiyoku H, Saibara T, Onishi S. Development of hepatic sinusoidal structure with special reference to the Ito cells. Microsc Res Tech 1997;39:336–349.
32. Tazaki T, Miyazaki K, Hiyama E, Nakamoto T, Sakai R, Yamasaki N, et al. Functional analysis of Src homology 3-encoding exon (exon 2) of p130Cas in primary fibroblasts derived from exon 2-specific knockout mice. Genes Cells 2008;13:145–157.
33. Iwahara T, Akagi T, Fujitsuka Y, Hanafusa H. CrkII regulates focal adhesion kinase activation by making a complex with Crk-associated substrate, p130Cas. Proc Natl Acad Sci U S A 2004;101:17693–17698.
34. Shin NY, Dise RS, Schneider-Mergener J, Ritchie MD, Kilkenny DM, Hanks SK. Subsets of the major tyrosine phosphorylation sites in Crk-associated substrate (CAS) are sufficient to promote cell migration. J Biol Chem 2004;279:38331–38337.
35. Steffan AM, Gendrault JL, Kirn A. Increase in the number of fenestrae in mouse endothelial liver cells by altering the cytoskeleton with cytochalasin B. HEPATOLOGY 1987;7:1230–1238.
36. Braet F, De Zanger R, Jans D, Spector I, Wisse E. Microfilament-disrupting agent latrunculin A induces and increased number of fenestrae in rat liver sinusoidal endothelial cells: comparison with cytochalasin B. HEPATOLOGY 1996;24:627–635.
37. Braet F, Spector I, De Zanger R, Wisse E. A novel structure involved in the formation of liver endothelial cell fenestrae revealed by using the actin inhibitor misakinolide. Proc Natl Acad Sci U S A 1998;95: 13635–13640.
38. Braet F, Spector I, Shochet N, Crews P, Higa T, Menu E, et al. The new anti-actin agent dihydrohalichondramide reveals fenestrae-forming centers in hepatic endothelial cells. BMC Cell Biol 2002;3:1–14.
39. Yokomori H, Yoshimura K, Funakoshi S, Nagai T, Fujimaki K, Nomura M, et al. Rho modulates hepatic sinusoidal endothelial fenestrae via regulation of the actin cytoskeleton in rat endothelial cells. Lab Invest 2004;84:857–864.
40. Yokomori H, Yoshimura K, Nagai T, Fujimaki K, Nomura M, Hibi T, et al. Sinusoidal endothelial fenestrae organization regulated by myosin light chain kinase and Rho-kinase in cultured rat sinusoidal endothelial cells. Hepatol Res 2004;30:169–174.
41. Yokomori H, Oda M, Yoshimura K, Nagai T, Ogi M, Nomura M, et al. Vascular endothelial growth factor increases fenestral permeability in hepatic sinusoidal endothelial cells. Liver Int 2003;23:467–475.
42. Carpenter B, Lin Y, Stoll S, Raffai RL, McCuskey R, Wang R. VEGF is crucial for the hepatic vascular development required for lipoprotein uptake. Development 2005;132:3293–3303.
43. Yoshida M, Nishikawa Y, Omori Y, Yoshioka T, Tokairin T, McCourt P, et al. Involvement of signaling of VEGF and TGF-beta in differentiation of sinusoidal endothelial cells during culture of fetal rat liver cells. Cell Tissue Res 2007;392:273–282.
44. Yokomori H, Oda M, Ogi M, Yoshimura K, Nomura M, Fujimaki K, et al. Endothelin-1 suppresses plasma membrane Ca++-ATPase, concomitant with contraction of hepatic sinusoidal endothelial fenestrae. Am J Pathol 2003;162:557–566.
45. Yokomori H, Yoshimura Y, Ohshima S, Nagai T, Fujimaki K, Nomura M, et al. The endothelin-1 receptor-mediated pathway is not involved in the endothelin-1-induced defenestration of liver sinusoidal endothelial cells. Liver Int 2006;126:1268–1276.

46. Watanabe N, Takashimizu S, Nishizaki Y, Kojima S, Kagawa T, Matsuzaki S. An endothelin A receptor antagonist induces dilatation of sinusoidal endothelial fenestrae: implications for endothelin-1 in hepatic microcirculation. J Gastroenterol 2007;42:775–782.
47. Avraham HK, Lee TH, Koh Y, Kim TA, Jiang S, Sussman M, et al. Vascular endothelial growth factor regulates focal adhesion assembly in human brain microvascular endothelial cells through activation of the focal adhesion kinase and related adhesion focal tyrosine kinase. J Biol Chem 2003;278:36661–36668.
48. Casamassima A, Rozengurt E. Tyrosine phosphorylation of p130(cas) by bombesin, lysophosphatidic acid, phorbol esters, and platelet-derived growth factor. Signaling pathways and formation of a p130(cas)-Crk complex. J Biol Chem 1997;272:9363–9370.
49. Kim JT, Joo CK. Involvement of cell-cell interactions in the rapid stimulation of Cas tyrosine phosphorylation and Src kinase activity by transforming growth factor-beta 1. J Biol Chem 2002;277: 31938–31948.
50. Horn T, Christoffersen P, Henriksen JH. Alcoholic liver injury: defenestration in noncirrhotic livers—a scanning electron microscopic study. HEPATOLOGY 1987;7:77–82.
51. Xu GF, Wang XY, Ge GL, Li PT, Jia X, Tian DL, et al. Dynamic changes of capillarization and peri-sinusoid fibrosis in alcoholic liver diseases. World J Gastroenterol 2004;10:238–243.
52. Mori T, Okanoue T, Sawa Y, Hori N, Ohta M, Kagawa K. Defenestration of the sinusoidal endothelial cell in a rat model of cirrhosis. HEPATOLOGY 1993;17:891–897.
53. Xu B, Broome U, Uzunel M, Nava S, Ge X, Kumagai-Braesch M, et al. Capillarization of hepatic sinusoid by liver endothelial cell-reactive autoantibodies in patients with cirrhosis and chronic hepatitis. Am J Pathol 2003;163:1275–1289.
54. Ichida T, Hata K, Yamada S, Hatano T, Miyagiwa M, Miyabayashi C, et al. Subcellular abnormalities of liver sinusoidal lesions in human hepatocellular carcinoma. J Submicrosc Cytol Pathol 1990;22:221–229.
55. Kin M, Torimura T, Ueno T, Inuzuka S, Tanikawa K. Sinusoidal capillarization in small hepatocellular carcinoma. Pathol Int 1995;44: 771–778.
56. Xu H, Shi BM, Lu XF, Liang F, Jin X, Wu TH, et al. Vascular endothelial growth factor attenuates hepatic sinusoidal capillarization in thioacetamide-induced cirrhotic rats. World J Gastroenterol 2008;14: 2349–2357.

Cancer Letters 297 (2010) 220–225

Contents lists available at ScienceDirect

Cancer Letters

journal homepage: www.elsevier.com/locate/canlet

All-trans retinoic acid downregulates ALK in neuroblastoma cell lines and induces apoptosis in neuroblastoma cell lines with activated ALK

Hitoyasu Futami, Ryuichi Sakai *

Growth Factor Division, National Cancer Center Research Institute, 5-1-1, Tsukiji-, Chuo-ku, Tokyo 104-0045, Japan

ARTICLE INFO

Article history:
Received 21 January 2010
Received in revised form 2 May 2010
Accepted 18 May 2010

Keywords:
ALK
ATRA
Neuroblastoma

ABSTRACT

Recently, gene amplification and gain-of-function mutations of ALK have been found in some neuroblastoma cell lines and clinical tumor samples. We have previously reported that knockdown of ALK by RNAi induced apoptosis in neuroblastoma cells with gene amplification of ALK. We report that all-trans retinoic acid (ATRA) downregulates ALK in neuroblastoma cell lines. Downregulation of ALK protein by ATRA was accompanied by apoptosis in neuroblastoma cells with gene amplification or gain-of-function mutation of ALK but not in neuroblastoma cells without these genetic alterations. These results suggest that ALK downregulation by ATRA might lead to apoptosis in neuroblastoma cells with activated ALK.

© 2010 Elsevier Ireland Ltd. All rights reserved.

1. Introduction

Neuroblastoma is a pediatric solid tumor derived from the sympathoadrenal lineage of the neural crest and is responsible for approximately 15% of all cancer deaths in children [1]. Although improvement of multimodal therapy has been achieved by the progress of treatment, prognosis of this cancer, especially high-risk neuroblastoma, remains poor.

Retinoic acids have been reported to exhibit *in vitro* growth-inhibitory effect and differentiation on neuroblastoma cells as well as *in vivo* anti-tumor activity [2–4] and have been used in the treatment of neuroblastoma patients [5]. Currently, 13-cis retinoic acid is an established component of the treatment combined with myeloablative therapy and autologous bone-marrow transplantation in high-risk neuroblastoma patients [6,7]. Although the mechanism of anti-tumor effect of retinoic acids has not yet been fully elucidated, it has been suggested that induction of differentiation or apoptosis might contribute to the therapeutic effect of retinoic acids against human neuroblastomas [8–11].

ALK was originally identified in anaplastic large cell lymphomas as a novel protein tyrosine kinase that forms an oncogenic fusion product with the NPM nucleolar phosphoprotein by chromosomal translocation [12,13]. ALK has also been found to be fused with a variety of partners in human cancers including inflammatory myofibroblastic tumors [14], esophageal cancer [15], and non-small cell lung cancer [16,17]. We have previously reported that somatically acquired amplification of ALK occurs in the neuroblastoma cell lines and tumors of neuroblastoma patients [18,19]. Subsequently, both the germline and somatic gain-of-function mutations of ALK were recently found in familial and sporadic neuroblastoma patients, respectively [20–23]. It was demonstrated that, in the neuroblastoma cell lines exhibiting gene amplification or harboring gain-of-function mutations of ALK, knockdown of ALK by RNAi or an ALK inhibitor induced apoptosis and inhibition of cell growth, suggesting that ALK plays an important role in the pathogenesis of neuroblastoma [19–23].

In this study, we found all-trans retinoic acid (ATRA), one of retinoic acids, downregulated ALK expression in neuroblastoma cell lines. Since it is considered that inhibition of the activated oncogene product might have a great impact on the biological property of neuroblastoma cells,

* Corresponding author. Tel.: +81 03 3542 2511; fax: +81 03 3542 8170.
E-mail address: rsakai@ncc.go.jp (R. Sakai).

0304-3835/$ - see front matter © 2010 Elsevier Ireland Ltd. All rights reserved.
doi:10.1016/j.canlet.2010.05.014

we further examined whether the suppression of ALK by ATRA caused the biological effect of apoptosis induction and growth inhibition in neuroblastoma cells in an association with the presence of activation of ALK.

2. Materials and methods

2.1. Cell line and culture

NB-39-nu, SH-SY5Y, TNB-1, and GOTO neuroblastoma cell lines were maintained in RPMI 1640 medium with 10% heat-inactivated fetal bovine serum (FBS), 100 units/ml of penicillin and 100 μg/ml of streptomycin at 37 °C with 5% CO_2.

2.2. Antibodies for Western blotting

Anti-ALK antibody was prepared as previously described [18]. Anti-cleaved caspase-3 antibody, anti-phospho-ERK1/2 antibody (phospho-p44/p42 mitogen-activated protein kinase [MAPK] antibody), anti-AKT antibody, anti-phospho-AKT (Ser473) antibody were purchased from Cell Signaling (Danvers, MA, USA), and anti-β-actin (I-19) antibody were purchased from Santa Cruz Biotechnology (Santa Cruz, CA, USA).

2.3. Western blotting

The cell lysates were separated on sodium dodecyl sulfate–polyacrylamide gel electrophoresis, and transferred to a polyvinylidene difluoride membrane (Immobilon-P; Millipore Corporation, Bedford, MA, USA). After blocking of the membrane with blocking buffer (Blocking One; Nacalai Tesque, Kyoto, Japan), the membrane was probed with antibodies for detection. The membrane was further probed with HRP-conjugated anti-rabbit or anti-mouse IgG to visualize the reacted antibody.

2.4. Apoptosis assay

Apoptosis levels were determined using Cell Death Detection ELISA kit (Roche Diagnostics, Mannheim, Germany), which detects the presence of nucleosomes in the cytoplasm of apoptotic cells. Briefly, cells were seeded in 96-well plates (Becton Dickinson, NJ, USA), cultured with dimethylsulfoxide (DMSO) or ATRA (Sigma, St. Louis, MO, USA) in RPMI 1640 medium with 10% heat-inactivated fetal bovine serum (FBS), 100 units/ml of penicillin and 100 μg/ml of streptomycin at 37 °C with 5% CO_2, then subjected to Cell Death Detection ELISA kit according to the manufacturer's instructions. The absorbance of the samples was measured at a wavelength of 405 nm using a microplate reader mode 550 (Bio-Rad, Hercules, CA, USA).

2.5. Cell growth assay

Cell growth was analyzed by Tetra Color One (Seikagaku, Tokyo, Japan) according to the manufacturer's instructions. Briefly, cells were seeded in 96-well plates (Beckton Dickinson, NJ), cultured with DMSO or ATRA in RPMI 1640 medium with 10% heat-inactivated FBS, 100 units/ml of penicillin and 100 μg/ml of streptomycin at 37 °C with 5% CO_2, then subjected to Tetra Color one for 3 h followed by measurement for cell growth. The absorbances of the samples were measured at 450 nm on a microplate reader mode 550 (Bio-Rad, Hercules, CA, USA).

2.6. Quantitative real-time RT-PCR

Total RNA was isolated using ISOGEN (Nippon gene, Toyama, Japan). For reverse transcription, AccuScript High Fidelity 1st Strand cDNA Synthesis kit (Stratagene, La Jolla, CA, USA) was used and quantitative real-time PCR was performed in Fluorescent Quantitative Detection System Line-Gene (BioFlux, Tokyo, Japan) using QantiTect SYBER Green PCR kit (Qiagen, Tokyo, Japan). Relative abundance of the specific mRNAs was normalized to GAPDH mRNA. The following primer sets were used for quantitative real-time RT-PCR: ALK; forward, 5′-ACCACTTCATCCACCGAGGC-3′ and reverse, 5′-CAGGGTCCTTGGGCCTCACA-3′. GAPDH; forward, 5′- TGAAGGTCGGTGTCAACGGATTTGGC-3′ and reverse, 5′-CATGTAGGCCATGAGGTCCACCAC-3′.

3. Results

3.1. ATRA suppressed the expression of ALK protein in various neuroblastoma cell lines

We first examined the level of ALK protein in four neuroblastoma cell lines growing in culture medium. As previously reported [18], the level of ALK protein was extremely high in NB-39-nu cells when compared with that in SH-SY5Y, TNB-1 and GOTO cells (Fig. 1A). We next examined whether ATRA affected the protein expression level of ALK in these four neuroblastoma cell lines. When the four cell lines were treated with ATRA at the concentration of 1 μM or 10 μM for 72 h, the levels of ALK protein were remarkably reduced in all cell lines examined regardless of the original levels of expression (Fig. 1B). The reduction of ALK protein expression at 24 h after ATRA treatment was not obvious, suggesting that this reduction is a rather slow process that occurs around 1 day after the treatment (data not shown).

3.2. Inhibition of mRNA expression by treatment with ATRA in NB-39-nu neuroblastoma cells

Since the protein expression levels of ALK were reduced in four neuroblastoma cells treated with ATRA, mRNA expression levels in neuroblastoma cells treated with ATRA were analyzed for NB-39-nu cells using quantitative real-time RT-PCR. As shown in Fig. 2, quantitative levels of ALK mRNA of the NB-39-nu cells were reduced at 24 h after the treatment with ATRA at the concentration of 1 μM and 10 μM, indicating that ATRA inhibited mRNA expression of ALK.

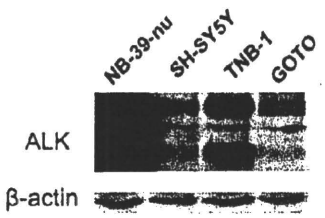

Fig. 1A. ALK protein expression in NB-39-nu, SH-SY5Y, TNB-1 and GOTO neuroblastoma cells. Cell lysates obtained from NB-39-nu, SH-SY5Y, TNB-1 and GOTO cells growing in RPMI 1640 medium with 10% FBS were subjected to Western blotting analysis with anti-ALK antibody and anti-β-actin.

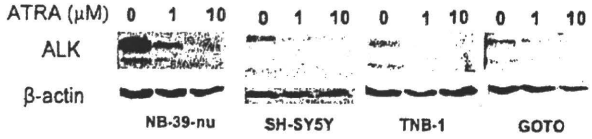

Fig. 1B. Downregulation by all-trans retinoic acid (ATRA) in NB-39-nu, SH-SY5Y, TNB-1 and GOTO neuroblastoma cells. NB-39-nu, SH-SY5Y, TNB-1 and GOTO cells were cultured with DMSO (vehicle) or ATRA (1 μM, 10 μM) in RPMI 1640 medium with 10% FBS for 72 h in a 6-well plate (15,000–30,000/ml, 3 ml/well) after preincubation for 24 h and harvested for cell lysate preparation. The cell lysates were subjected to Western blotting with anti-ALK antibody and anti-β-actin.

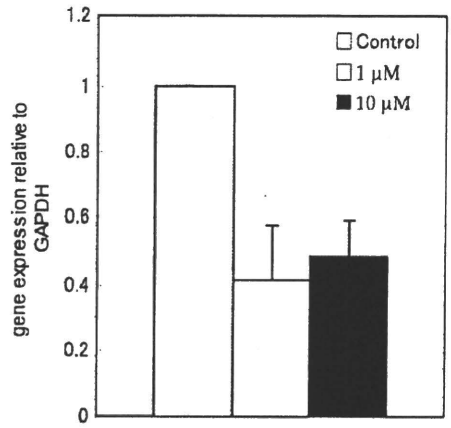

Fig. 2. Quantitative analysis of mRNA expression in NB-39-nu neuroblastoma cells treated with ATRA. NB-39-nu cells were cultured in a 6-well plate with DMSO (vehicle) or ATRA (1 μM, 10 μM) in RPMI 1640 medium with 10% FBS for 24 h after preincubation for 24 h, and then harvested for isolation of total RNA. The samples were subjected to quantification of ALK mRNA using real-time quantitative RT-PCR as described in Section 2. Columns, mean of three replicate; bars, SD.

3.3. ATRA induced apoptosis in NB-39-nu and SH-SY5Y neuroblastoma cell lines with activated ALK but not TNB-1 and GOTO neuroblastoma cell lines without activated ALK

It was previously reported that knockdown of ALK by RNAi or treatment with an ALK inhibitor induced apoptosis and inhibited cell growth in neuroblastoma cell lines in which ALK was activated by gene amplification or gain-of-function mutations. Therefore, we next examined whether apoptosis was induced by treatment with ATRA in neuroblastoma cell lines with activated ALK. As previously reported [18,21], NB-39-nu and SH-SY5Y cell lines harbor gene amplification and gain-of-function of mutation of ALK, respectively. Apoptosis assay demonstrated that obvious apoptosis was detected in NB-39-nu and SH-SY5Y cells whereas it was not observed in TNB-1 and GOTO cells (Fig. 3). It was of note that apoptosis was induced in the cells with ALK gene amplification or gain-of-function mutation but not in the cells without the genetic alteration of ALK. Reduction of the apoptosis value in the SH-SY5Y cells treated with 10 μM ATRA compared to that with 1 μM ATRA appeared to be due to extensive cell death. We next tested whether apoptosis was induced by detection of cleaved caspase-3 using the anti-cleaved caspase-3 antibody. The analysis demonstrated that cleaved caspase-3 was detected in NB-39-nu and SH-SY5Y cells by 72 h treatment with ATRA, whereas it was not detected in TNB-1 and GOTO cells (Fig. 4). This result was consistent with the results obtained by the apoptosis assay described above.

3.4. Effect of ATRA on AKT/ERK signaling pathways in NB-39-nu neuroblastoma cells

We subsequently investigated status of AKT/ERK signaling pathways in NB-39-nu cells after the treatment with ATRA to examine whether upstream of anti-apoptotic signaling were affected. Western blotting showed that phosphorylation of AKT and ERK after 48 h treatment with ATRA were suppressed, indicating that AKT/ERK signaling pathways were inhibited by the treatment with ATRA (Fig. 5).

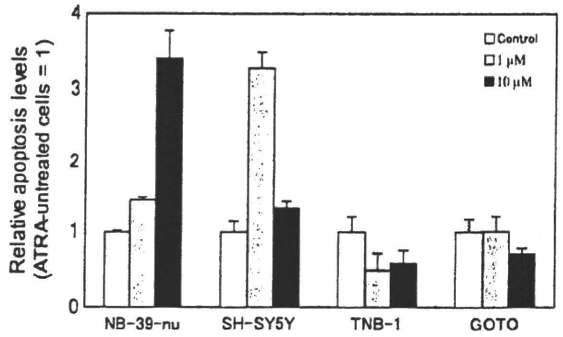

Fig. 3. Effect of ATRA on the induction of apoptosis in NB-39-nu, SH-SY5Y, TNB-1 and GOTO neuroblastoma cells. NB-39-nu, SH-SY5Y, TNB-1 and GOTO cells were incubated for 72 h in a 96-well plate (15,000–30,000 cells/ml, 0.1 ml/well) with DMSO (vehicle) or ATRA (1 μM, 10 μM) in RPMI 1640 medium with 10% FBS after preincubation for 24 h, and then subjected to the apoptosis assay using Cell Death Detection ELISA kit as described in Section 2. Columns, means of three replicates; bars, SD.

3.5. Effect of ATRA on cell growth of NB-39-nu, SH-SY5Y, TNB-1, and GOTO neuroblastoma cells

We next examined whether cell growth of NB-39-nu and SH-SY5Y cells that underwent ATRA-induced apoptosis was inhibited by the treatment with ATRA. Analysis by Tetra Color One assay demonstrated that the cell growth of these cells was inhibited by the treatment with ATRA (Fig. 6). Cell growth of TNB-1 and GOTO cells, which did not show significant apoptosis by ATRA, was also inhibited by treatment with ATRA (Fig. 6). As demonstrated by Fig. 7C, TNB-1 cells treated with ATRA showed neurite outgrowth, suggesting the induction of differentiation, which might contribute to the inhibition of cell growth. GOTO cells, however, did not obviously show neurite outgrowth from the morphological appearance (Fig. 7D).

4. Discussion

In this study, we found that treatment by ATRA caused remarkable downregulation of ALK protein in neuroblastoma cell lines. This is the first report that retinoic acid can suppress the expression of ALK, which is an oncogenic protein recently found in several cancers including neuroblastoma. Since retinoic acids are known to regulate the transcription of a number of genes, we examined whether ATRA had some effect on the ALK mRNA expression level. The treatment with ATRA reduced the mRNA level of ALK as shown by real-time quantitative RT-PCR, suggesting that the transcriptional suppression of ALK mRNA by ATRA contributed to the downregulation of ALK protein.

Although the significant suppression of ALK protein expression by ATRA was observed in all cell lines examined, apoptosis was shown only in the cell lines with gene amplification or a gain-of-function mutation of ALK. Most SH-SY5 cells died and turned into fragments by treatment of 10 μM ATRA (data not shown). This massive cell death appeared to have resulted in a relatively low apoptosis level in this assay although the apoptosis level was significantly elevated even at 1 μM of ATRA. Judging from samples harvested from supernatant of the cells treated with 10 μM of ATRA, at least about 30% and 70% of the cell

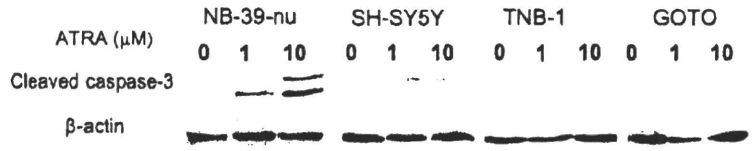

Fig. 4. Analysis for detection of cleaved caspase-3 in NB-39-nu, SH-SY5Y, TNB-1 and GOTO neuroblastoma cells by treatment with ATRA. NB-39-nu, SH-SY5Y, TNB-1 and GOTO cells were cultured with ATRA in 6-well plate cells (15,000–30,000 cells/ml, 3 ml/well) with DMSO (vehicle) or ATRA (1 μM, 10 μM) in RPMI 1640 medium with 10% FBS for 72 h after preincubation for 24 h and harvested for cell lysate preparation. The cell lysates were subjected to Western blotting with anti-cleaved caspase-3 antibody and anti-β-actin.

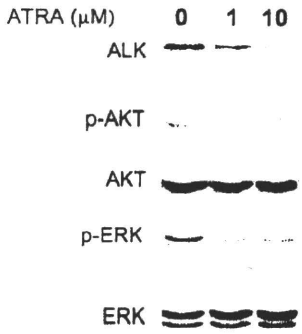

Fig. 5. Effect of ATRA on AKT/ERK signaling pathways in NB-39-nu neuroblastoma cells. NB-39-nu or ATRA (1 μM, 10 μM) in RPMI 1640 medium with 10% FBS for 48 h in 6-well plates (20,000 cells/ml, 3 ml/well) after preincubation for 24 h and harvested for cell lyasate preparation. The cell lysates were subjected to Western blotting with anti-ALK antibody, anti-ERK1/2 antibody, anti-phospho-ERK1/2 antibody anti-AKT antibody, and anti-phospho-AKT antibody.

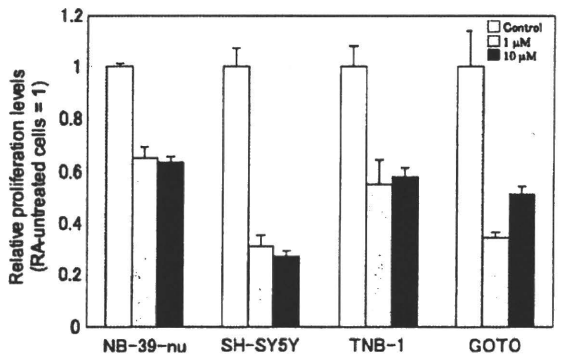

Fig. 6. Effect of ATRA on cell growth in NB-39-nu, SH-SY5Y, TNB-1 and GOTO neuroblastoma cells. NB-39-nu, SH-SY5Y, TNB-1 and GOTO cells were incubated in 96-well plates (7000–30,000 cells/ml, 0.1 ml/well) with DMSO (vehicle) or ATRA (1 μM, 10 μμMM) in RPMI 1640 medium with 10% FBS after preincubation for 24 h. The treatment time with ATRA was 120 h for NB-39-nu cells, and 72 h for SH-SY5Y, TNB-1 and GOTO cells. Cell growth was determined by Tetra Color One assay as described in Section 2. Columns, means of three replicates; bars, SD.

appeared to have died due to apoptosis in NB-30-nu and SH-SY5Y cells, respectively, while less than 1% of each cells in TNB-1 cells and GOTO cells did. In NB-39-nu cells, which were demonstrated to have gene amplification of ALK [18], we previously showed induction of apoptosis by treatment with ALK siRNA [19]. The degree of downregulation of ALK, which had been caused by treatment with ALK RNAi, was almost as remarkable as that by the treatment with ATRA, which caused apoptosis in NB-39-nu cells in this study [19]. It was also reported that the suppression of ALK by RNAi or an ALK inhibitor induced apoptosis and inhibited cell proliferation in the neuroblastoma cell lines harboring gain-of-function mutations of ALK such as SH-SY5Y cells [20–23]. These findings suggest that the survival of neuroblastoma cell lines with activated ALK is dependent on the presence of activated ALK gene product, being consistent with the phenomenon of "oncogene addiction," which describes the acquired dependence of tumor cells on an activated oncogene for their survival and/or proliferation [17]. Thus, it is likely that the induction of apoptosis by ATRA treatment in neuroblastoma cells harboring activated ALK might be caused at least in part by the reduction of ALK expression by ATRA, although it might be led by other molecular mechanisms regulating ATRA-induced apoptosis in an ALK-independent manner.

We previously demonstrated that inhibition of ALK expression by RNAi for ALK caused inhibition of AKT/ERK pathways and apoptosis induction in NB-39-nu cells [19]. In the current study, we also observed that AKT/ERK signaling pathways were suppressed when the expression of ALK was inhibited by the treatment with ATRA, suggesting that the inhibition of ALK by ATRA lead to the inhibition of anti-apoptotic signaling pathways via suppression of AKT/ERK pathways and was enough to cause apoptosis in NB-39-nu cells although it could be postulated that ATRA also affected other apoptosis-inducing signaling pathways as well.

It has been reported that retinoic acids downregulated expression of other oncogenic gene products such as MYCN in association with differentiation, apoptosis, and growth inhibition in various neuroblastoma cell lines. Although the possibility that reduction of those oncogenic gene expression might contribute to apoptosis induction could not be neglected since it is hard to examine the contribution of each target of ATRA for apoptosis in neurblastoma, we would insist in this study that the change in the ALK is so significant that it could affect the survival of ALK-addicted neuroblastoma cells.

Retinoic acids have been widely used in the treatment of various diseases including cancer [24]. In neuroblastomas, retinoic acids including ATRA, 13-cis retinoic acid, and other analogues have been employed alone or in combination with other modalities of chemotherapy and radiation for high-risk patients [5–7,25,26]. It was reported that neuroblastoma with mutated ALK accounted for 6.1–13.4% of neuroblastoma patients examined [20–23]. In addition, high-level gene amplification was observed in several percent of patients [19,21]. Thus, the total population of neuroblastoma patients with ALK mutation or gene amplification

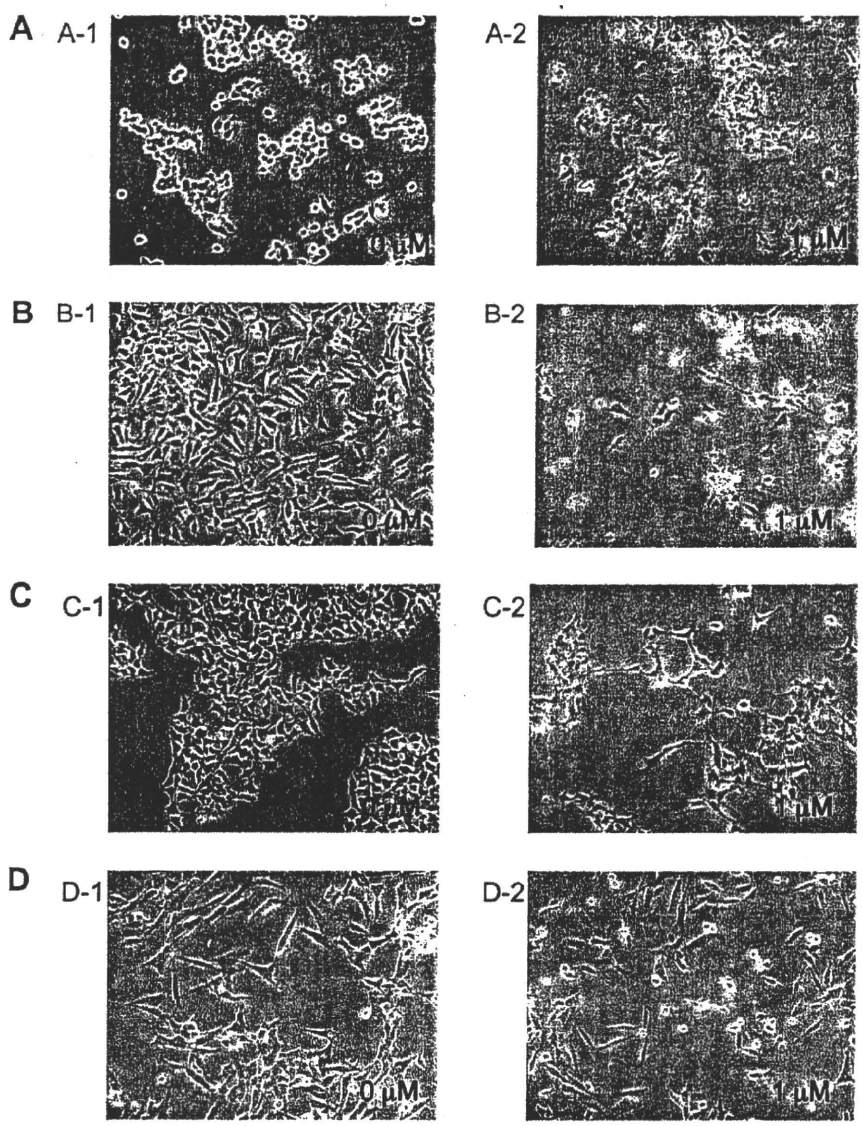

Fig. 7. Microscopic appearance of NB-39-nu, SH-SY5Y, TNB-1 and GOTO neuroblastoma cells treated with ATRA. NB-39-nu (A-1, -2), SH-SY5Y (B-1, -2), TNB-1 (C-1, -2) and GOTO (D-1, -2) cells were incubated with ATRA (0 μM, 1 μM) in RPMI 1640 medium with 10% FBS in 6-well plate cells (15,000–30,000 cells/ml, 3 ml/well) after preincubation for 24 h, and then photographed. The treatment with ATRA was 120 h for NB-39-nu cells, and 72 h for SH-SY5Y, TNB-1 and GOTO cells.

is about 10%. Therefore, some patients with activated ALK might have exhibited good clinical response due to the reduction of activated ALK by retinoic acid among neuroblastoma patients who received successful treatment with retinoic acid although this population needs to be identified by a clinical investigation. A subset of these neuroblastoma patients with activated ALK might be an even more appropriate candidate for the use of retinoic acids.

Conflicts of interest

No potential conflicts of interest were disclosed.

Acknowledgements

This work was supported by a Grant-in Aid for Cancer Research by the Ministry of Education, Culture, Sports, Science and Technology of Japan and in part by a Grant-in-Aid from the Ministry of Health, Labor and Welfare of Japan for the 3rd-term Comprehensive 10-year Strategy for Cancer Control.

We thank Dr. Toshihiko Tsukada for technical instruction on the Fluorescent Quantitative Detection System LineGene.

References

[1] J.M. Maris, K.K. Matthay, Molecular biology of neuroblastoma, J. Clin. Oncol. 17 (1999) 2264–2279.
[2] N. Sidell, Retinoic acid-induced growth inhibition and morphologic differentiation of human neuroblastoma cells in vitro, J. Natl. Cancer Inst. 68 (1982) 589–596.
[3] C.J. Thiele, C.P. Reynolds, M.A. Israel, Decreased expression of N-myc precedes retinoic acid-induced morphological differentiation of human neuroblastoma, Nature 313 (1985) 404–406.
[4] E. Abemayor, B. Chang, N. Sidell, Effects of retinoic acid on the in vivo growth of human neuroblastoma cells, Cancer Lett. 55 (1990) 1–5.

[5] C.P. Reynolds, K.K. Matthay, J.G. Villablanca, B.J. Maurer, Retinoid therapy of high-risk neuroblastoma, Cancer Lett. 197 (2003) 185–192.
[6] K.K. Matthay, J.G. Villablanca, R.C. Seeger, D.O. Stram, R.E. Harris, N.K. Ramsay, P. Swift, H. Shimada, C.T. Black, G.M. Brodeur, R.B. Gerbing, C.P. Reynolds, Treatment of high-risk neuroblastoma with intensive chemotherapy, radiotherapy, autologous bone marrow transplantation, and 13-cis-retinoic acid, Children's Cancer Group, New Engl. J. Med. 341 (1999) 1165–1173.
[7] K.K. Matthay, C.P. Reynolds, R.C. Seeger, H. Shimada, E.S. Adkins, D. Haas-Kogan, R.B. Gerbing, W.B. London, J.G. Villablanca, Long-term results for children with high-risk neuroblastoma treated on a randomized trial of myeloablative therapy followed by 13-cis-retinoic acid: a children's oncology group study, J. Clin. Oncol. 27 (2009) 1007–1013.
[8] M. Ponzoni, P. Bocca, V. Chiesa, A. Decensi, V. Pistoia, L. Raffaghello, C. Rozzo, P.G. Montaldo, Differential effects of N-(4-hydroxyphenyl)retinamide and retinoic acid on neuroblastoma cells: apoptosis versus differentiation, Cancer Res. 55 (1995) 853–861.
[9] G. Melino, C.J. Thiele, R.A. Knight, M. Piacentini, Retinoids and the control of growth/death decisions in human neuroblastoma cell lines, J. Neurooncol. 31 (1997) 65–83.
[10] A. Voigt, F. Zintl, Effects of retinoic acid on proliferation, apoptosis, cytotoxicity, migration, and invasion of neuroblastoma cells, Med. Pediatr. Oncol. 40 (2003) 205–213.
[11] H. Niizuma, Y. Nakamura, T. Ozaki, H. Nakanishi, M. Ohira, E. Isogai, H. Kageyama, M. Imaizumi, A. Nakagawara, Bcl-2 is a key regulator for the retinoic acid-induced apoptotic cell death in neuroblastoma, Oncogene 25 (2006) 5046–5055.
[12] M. Shiota, J. Fujimoto, T. Semba, H. Satoh, T. Yamamoto, S. Mori, Hyperphosphorylation of a novel 80 kDa protein-tyrosine kinase similar to Ltk in a human Ki-1 lymphoma cell line, AMS3, Oncogene 9 (1994) 1567–1574.
[13] S.W. Morris, M.N. Kirstein, M.B. Valentine, K.G. Dittmer, D.N. Shapiro, D.L. Saltman, A.T. Look, Fusion of a kinase gene, ALK, to a nucleolar protein gene, NPM, in non-Hodgkin's lymphoma, Science 263 (1994) 1281–1284.
[14] C.A. Griffin, A.L. Hawkins, C. Dvorak, C. Henkle, T. Ellingham, E.J. Perlman, Recurrent involvement of 2p23 in inflammatory myofibroblastic tumors, Cancer Res. 59 (1999) 2776–2780.
[15] F.R. Jazii, Z. Najafi, R. Malekzadeh, T.P. Conrads, A.A. Ziaee, C. Abnet, M. Yazdznbod, A.A. Karkhane, G.H. Salekdeh, Identification of squamous cell carcinoma associated proteins by proteomics and loss of beta tropomyosin expression in esophageal cancer, World J. Gastroenterol. 12 (2006) 7104–7112.
[16] K. Rikova, A. Guo, Q. Zeng, A. Possemato, J. Yu, H. Haack, J. Nardone, K. Lee, C. Reeves, Y. Li, Y. Hu, Z. Tan, M. Stokes, L. Sullivan, J. Mitchell, R. Wetzel, J. Macneill, J.M. Ren, J. Yuan, C.E. Bakalarski, J. Villen, J.M. Kornhauser, B. Smith, D. Li, X. Zhou, S.P. Gygi, T.L. Gu, R.D. Polakiewicz, J. Rush, M.J. Comb, Global survey of phosphotyrosine signaling identifies oncogenic kinases in lung cancer, Cell 131 (2007) 1190–1203.
[17] M. Soda, Y.L. Choi, M. Enomoto, S. Takada, Y. Yamashita, S. Ishikawa, S. Fujiwara, H. Watanabe, K. Kurashina, H. Hatanaka, M. Bando, S. Ohno, Y. Ishikawa, H. Aburatani, T. Niki, Y. Sohara, Y. Sugiyama, H. Mano, Identification of the transforming EML4-ALK fusion gene in non-small-cell lung cancer, Nature 448 (2007) 561–566.
[18] I. Miyake, Y. Hakomori, A. Shinohara, T. Gamou, M. Saito, A. Iwamatsu, R. Sakai, Activation of anaplastic lymphoma kinase is responsible for hyperphosphorylation of ShcC in neuroblastoma cell lines, Oncogene 21 (2002) 5823–5834.
[19] Y. Osajima-Hakomori, I. Miyake, M. Ohira, A. Nakagawara, A. Nakagawa, R. Sakai, Biological role of anaplastic lymphoma kinase in neuroblastoma, Am. J. Pathol. 167 (2005) 213–222.
[20] Y. Chen, J. Takita, Y.L. Choi, M. Kato, M. Ohira, M. Sanada, L. Wang, M. Soda, A. Kikuchi, T. Igarashi, A. Nakagawara, Y. Hayashi, H. Mano, S. Ogawa, Oncogenic mutations of ALK kinase in neuroblastoma, Nature 455 (2008) 971–974.
[21] R.E. George, T. Sanda, M. Hanna, S. Frohling, W. Luther 2nd, J. Zhang, Y. Ahn, W. Zhou, W.B. London, P. McGrady, L. Xue, S. Zozulya, V.E. Gregor, T.R. Webb, N.S. Gray, D.G. Gilliland, L. Diller, H. Greulich, S.W. Morris, M. Meyerson, A.T. Look, Activating mutations in ALK provide a therapeutic target in neuroblastoma, Nature 455 (2008) 975–978.
[22] I. Janoueix-Lerosey, D. Lequin, L. Brugieres, A. Ribeiro, L. de Pontual, V. Combaret, V. Raynal, A. Puisieux, G. Schleiermacher, G. Pierron, D. Valteau-Couanet, T. Frebourg, J. Michon, S. Lyonnet, J. Amiel, O. Delattre, Somatic and germline activating mutations of the ALK kinase receptor in neuroblastoma, Nature 455 (2008) 967–970.
[23] Y.P. Mosse, M. Laudenslager, L. Longo, K.A. Cole, A. Wood, E.F. Attiyeh, M.J. Laquaglia, R. Sennett, J.E. Lynch, P. Perri, G. Laureys, F. Speleman, C. Kim, C. Hou, H. Hakonarson, A. Torkamani, N.J. Schork, G.M. Brodeur, G.P. Tonini, E. Rappaport, M. Devoto, J.M. Maris, Identification of ALK as a major familial neuroblastoma predisposition gene, Nature 455 (2008) 930–935.
[24] M.A. Smith, D.R. Parkinson, B.D. Cheson, M.A. Friedman, Retinoids in cancer therapy, J. Clin. Oncol. 10 (1992) 839–864.
[25] M.A. Smith, P.C. Adamson, F.M. Balis, J. Feusner, L. Aronson, R.F. Murphy, M.E. Horowitz, G. Reaman, G.D. Hammond, R.M. Fenton, et al., Phase I and pharmacokinetic evaluation of all-trans-retinoic acid in pediatric patients with cancer, J. Clin. Oncol. 10 (1992) 1666–1673.
[26] J.G. Villablanca, A.A. Khan, V.I. Avramis, R.C. Seeger, K.K. Matthay, N.K. Ramsay, C.P. Reynolds, Phase I trial of 13-cis-retinoic acid in children with neuroblastoma following bone marrow transplantation, J. Clin. Oncol. 13 (1995) 894–901.

Oncogene (2011) 30, 1413–1421
© 2011 Macmillan Publishers Limited All rights reserved 0950-9232/11
www.nature.com/onc

ORIGINAL ARTICLE

ARAP3 inhibits peritoneal dissemination of scirrhous gastric carcinoma cells by regulating cell adhesion and invasion

R Yagi[1], M Tanaka[1,2], K Sasaki[3], R Kamata[1], Y Nakanishi[4], Y Kanai[4] and R Sakai[1]

[1]Growth Factor Division and National Cancer Center Research Institute, Tsukiji, Tokyo, Japan; [2]Department of Molecular Medicine and Biochemistry, Akita University, School of Medicine, Hondo, Akita, Japan; [3]Department of Pharmacology, National Cerebral and Cardiovascular Center Research Institute, Suita, Osaka, Japan and [4]Pathology Division, National Cancer Center Research Institute, Tsukiji, Tokyo, Japan

During the analysis of phosphotyrosine-containing proteins in scirrhous gastric carcinoma cell lines, we observed an unusual expression of Arf-GAP with Rho-GAP domain, ankyrin repeat and PH domain 3 (ARAP3), a multimodular signaling protein that is a substrate of Src family kinases. Unlike other phosphotyrosine proteins, such as CUB domain-containing protein 1 (CDCP1) and Homo sapiens chromosome 9 open reading frame 10/oxidative stress-associated Src activator (C9orf10/Ossa), which are overexpressed and hyperphosphorylated in scirrhous gastric carcinoma cell lines, ARAP3 was underexpressed in cancerous human gastric tissues. In this study, we found that overexpression of ARAP3 in the scirrhous gastric carcinoma cell lines significantly reduced peritoneal dissemination. *In vitro* studies also showed that ARAP3 regulated cell attachment to the extracellular matrix, as well as invasive activities. These effects were suppressed by mutations in the Rho-GTPase-activating protein (GAP) domain or in the C-terminal two tyrosine residues that are phosphorylated by Src. Thus, the expression and phosphorylation state of ARAP3 may affect the invasiveness of cancer by modulating cell adhesion and motility. Our results suggest that ARAP3 is a unique Src substrate that suppresses peritoneal dissemination of scirrhous gastric carcinoma cells.

Oncogene (2011) **30,** 1413–1421; doi:10.1038/onc.2010.522; published online 15 November 2010

Keywords: ARAP3; scirrhous gastric carcinoma; Rho-GAP; cell-ECM adhesion; invasion

Introduction

The prognosis of scirrhous gastric carcinoma is poor because peritoneal dissemination and rapid submucosal invasion make it refractory to cancer treatments. Therefore, the discovery of novel therapeutic targets that control the progression of scirrhous gastric carcinoma is urgently needed. However, progress has been limited by the lack of knowledge about the factors and signaling pathways that mediate peritoneal dissemination and invasion.

Previous studies have shown that Src family tyrosine kinases (SFKs) are likely to be involved in these processes. For example, increased expression and kinase activity of SFKs frequently occurs during the transformation of precancerous cells (Frame, 2002). Activation of SFKs is also associated with tumor progression and metastasis, as well as with characteristic activities of cancer cells including proliferation, differentiation, motility, cell-extracellular matrix (ECM) adhesion, cell–cell adhesion and invasion (Brown and Cooper, 1996; Frame, 2002).

Recently, we reported that Src substrates such as CUB domain-containing protein 1 (CDCP1) (Uekita *et al.*, 2008) and Homo sapiens chromosome 9 open reading frame 10/oxidative stress-associated Src activator (C9orf10/Ossa) (Tanaka *et al.*, 2009) are hyperphosphorylated in the peritoneal nodules formed after inoculating the scirrhous gastric carcinoma cell line 44As3 into BALB/c nude mice. In our studies, we also detected another substrate of Src, Arf-GAP with Rho-GTPase-activated protein (GAP) domain, ankyrin repeat and PH domain 3 (ARAP3), in these nodules. However, immunohistochemical analysis showed that the expression level of ARAP3 was surprisingly higher in normal gastric glands than in cancerous tissue, unlike CDCP1 and C9orf10/Ossa.

ARAP3 functions as an effector of phosphoinositide 3-kinase (PI3K) by binding to phospatidyl-inositol-3,4,5-trisphosphate ($PI(3,4,5)P_3$) through pleckstrin homology (PH) domains (Krugmann *et al.*, 2002). On activation of PI3K signaling, ARAP3 is thought to be recruited to the plasma membrane, where it regulates lamellipodia formation and growth factor signaling (Kowanetz *et al.*, 2004; Krugmann *et al.*, 2004, 2006). ARAP3 is tyrosine-phosphorylated by Src mainly at the two tyrosine residues at the C-terminus (I *et al.*, 2004), whereas the biological role of tyrosine phosphorylation of ARAP3 is still unclear. In addition, the Rho-GAP domain of ARAP3 modulates the activity of Rho-family small GTPases, which regulate cytoskeletal dynamics as well as cancer invasion and metastasis. However, the

Correspondence: Dr R Sakai, Growth Factor Division, National Cancer Center Research Institute, 5-1-1 Tsukiji, Chuo-ku, Tokyo 104-0045, Japan.
E-mail: rsakai@ncc.go.jp
Received 1 June 2010; revised 10 September 2010; accepted 7 October 2010; published online 15 November 2010

relationship between these functions of ARAP3 and cancer phenotypes is not understood well.

In this study, we show that overexpression of ARAP3 in 58As9 cells, a highly metastatic scirrhous gastric carcinoma cell line, inhibited peritoneal dissemination in a mouse model. Furthermore, mutations to either the Rho-GAP domain or tyrosine phosphorylation sites of ARAP3 failed to inhibit peritoneal dissemination. ARAP3 also inhibited rapid cell-ECM adhesion and cell invasion *in vitro*. Our results support the hypothesis that ARAP3 suppresses the peritoneal dissemination of scirrhous gastric carcinoma cells.

Results

Expression of ARAP3 in human gastric tissues and tumor cell lines

Expression of ARAP3 in human gastric tissues was examined by immunohistochemical staining using an anti-ARAP3 antibody. ARAP3 is expressed primarily on the luminal side of the fundic gland (Figure 1a). In human gastric cancer tissues, ARAP3 expression was lower than in non-cancerous tissue (Figures 1b and c). Furthermore, the expression level of ARAP3 was lower in the undifferentiated type of gastric cancer than in the differentiated type (data not shown).

We also examined the expression of ARAP3 in 14 human gastric cancer cell lines (Figure 2). The expression of ARAP3 was very low or undetectable in 10 of these cell lines.

Roles of ARAP3 in peritoneal dissemination

To study the functional importance of ARAP3 in the peritoneal dissemination of scirrhous gastric carcinoma, we introduced ARAP3 expression vectors into 58As9 and NKPS scirrhous gastric carcinoma cell lines that expressed relatively little endogenous ARAP3 (Figure 2). Both the 58As9 and NKPS cell lines are highly metastatic (Yanagihara *et al*., 2005; Tanaka *et al*., 2009). After establishing 58As9 and NKPS cells that stably expressed wild-type ARAP3, we injected the cells into the peritoneal cavities of BALB/c nude mice (Figure 3 and Supplemental Figure 1). Compared with the parental 58As9 cell, the ARAP3-overexpressing cells formed fewer nodules on the mesentery and fatty tissues adjacent to the uterus (Figure 3b, lower panels). Essentially the same results were obtained from the analysis of ARAP3-expressing NKPS cells (Supplemental Figure 1B).

Effects of ARAP3 expression on the characteristics of gastric cancer cells in vitro

As the adhesiveness and invasiveness of scirrhous gastric carcinoma cell lines have a significant effect on peritoneal dissemination, we examined the effect of ARAP3 overexpression on the attachment of 58As9 cells to several ECM proteins, such as fibronectin, collagen

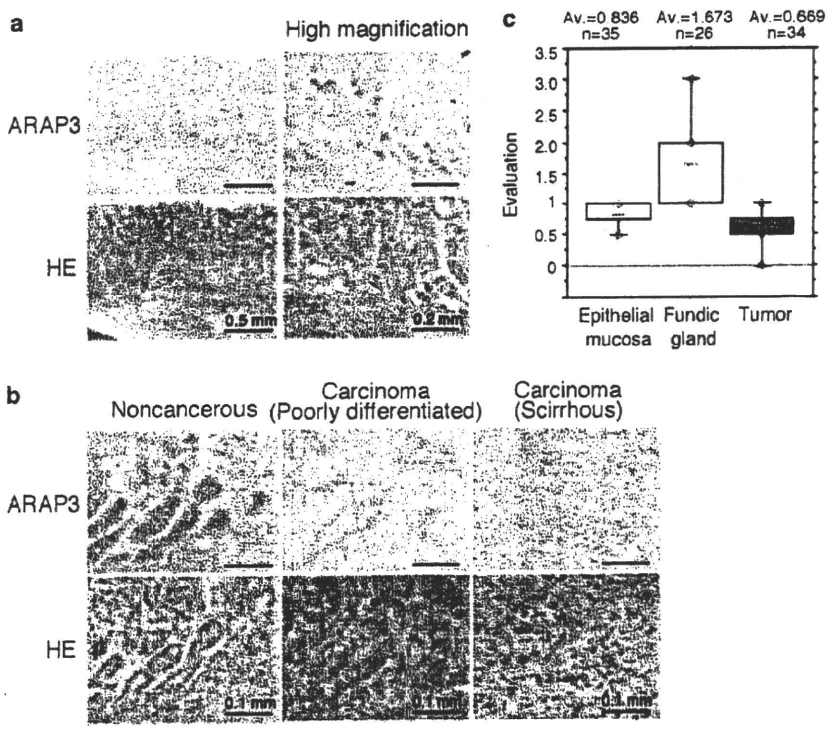

Figure 1 Immunohistochemical staining of ARAP3. Non-cancerous (**a**) and cancerous (**b**) human gastric tissues are shown. The intensity of staining was evaluated and arbitrarily scored from 0 to 3. The scores from samples of non-cancerous, cancerous and fundic gland tissues are shown in (**c**). Upper and lower quartiles are indicated with boxes, and minimum and maximum values are indicated with bars. Blue dots indicate the scores of all samples. Average scores (Av., red line) and sample numbers (n) are also shown. ARAP3 staining was detected in the fundic gland of the non-cancerous gastric tissues and was decreased in many cancerous tissues.

and vitronectin. Overexpression of ARAP3 partially suppressed the attachment of 58As9 cells to fibronectin and vitronectin (Figure 3c), but did not affect their adhesion to collagen. In addition, we performed an *in vitro* invasion assay using the 58As9 cell line with or without the overexpression of ARAP3. As shown in Figure 3d, ARAP3 clearly suppressed cell migration and invasion in 58As9 cells. ARAP3 also suppresses the cell migration activities and invasiveness of NKPS cells (Supplemental Figure 1C). However, overexpression of ARAP3 did not affect the cell growth (Supplemental Figure 2).

We also examined the effect of knocking down ARAP3 expression by using RNA interference in the 44As3 scirrhous gastric carcinoma cell line that expressed relatively high endogenous levels of ARAP3 (Figure 2a). ARAP3 expression was reduced in clones R3 and R5, as shown by immunoblotting (Figure 4A). Underexpression of ARAP3 promoted the attachment of 44As3 cells to fibronectin and vitronectin *in vitro* (Figure 4A). Moreover, an *ex vivo* adhesion assay, which measures the adhesiveness of gastric cancer cells to the mesothelium, showed the same results (Figure 4C). These results demonstrate that expression of ARAP3 may reduce the peritoneal dissemination of scirrhous gastric carcinoma cells by inhibiting cell-ECM adhesion and cell invasion. As activities of cell adhesion and invasion are strongly affected by morphological

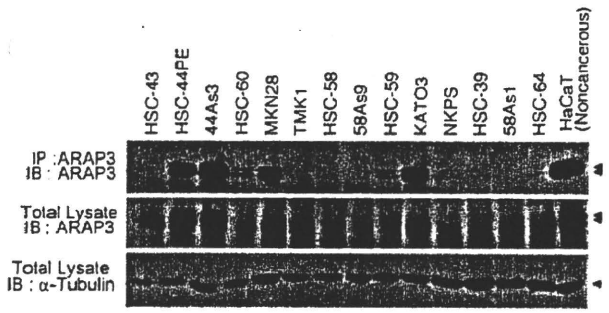

Figure 2 Expression of ARAP3 in human gastric cancer cell lines. Whole-cell lysates from non-scirrhous (MKN28, TMK1) and scirrhous human gastric cancer cell lines were immunoprecipitated with anti-ARAP3 antibody, and subsequently detected by immunoblotting. A human epithelial cell line, HaCaT, was used as a non-cancerous control. The expression of ARAP3 was diminished in 10 of the 14 gastric cancer cell lines tested.

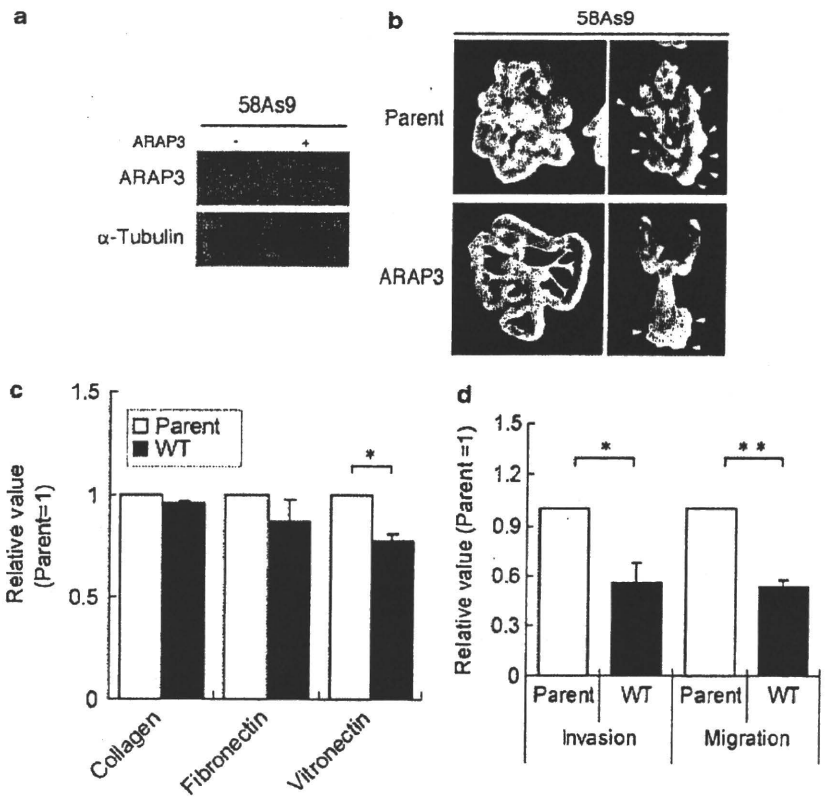

Figure 3 Functions of ARAP3 in the scirrhous gastric carcinoma cell line. The 58As9 cell line overexpressing ARAP3 was generated. Expression of ARAP3 was verified with immunoblotting (**a**). These cells were injected intraperitoneally into BALB/c nude mice ($n=4$). Mice were killed 21 days after injection and the peritoneal tissues were resected. (**b**) Tumors are indicated by yellow arrow heads. Cell adhesion to ECM proteins was also examined (**c**). Invasiveness was assessed *in vitro* by cell migration through a matrigel-coated or non-coated cell culture insert (**d**). ARAP3 expression suppressed cancerous activities of the scirrhous gastric carcinoma cell line *in vitro* and *in vivo* ($^*P<0.05$ $^{**}P<0.01$).

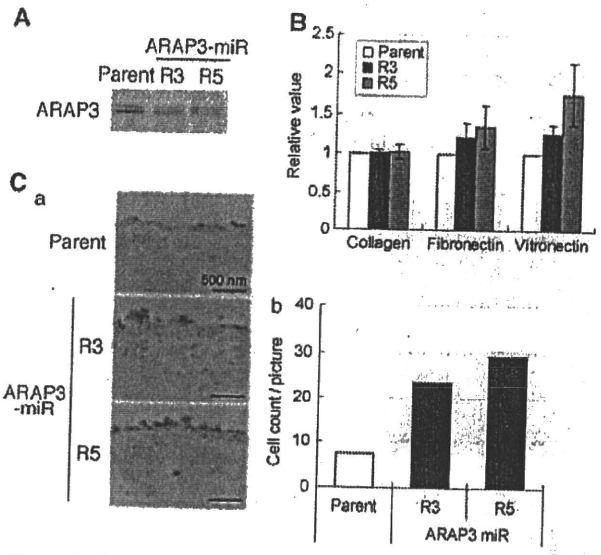

Figure 4 Expression of ARAP3 regulated cell-ECM attachment. ARAP3 was knocked down in 44As3 scirrhous gastric carcinoma cells by a microRNA knockdown system (R3 and R5 cells (A)). Cell attachment assays were performed with these cells *in vitro* (B) and *ex vivo* (C). In the *ex vivo* assay, the attachment of cancer cells to the mesentery was visualized by hematoxylin and eosin staining (C(a)) and quantified by cell counts (C(b)). Knockdown of ARAP3 increased the attachment of gastric carcinoma cells to both the ECM and mesentery.

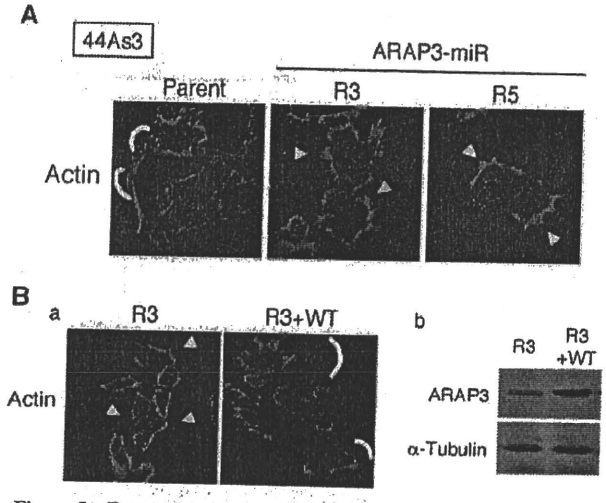

Figure 5 Expression of ARAP3 affected the morphology of the 44As3 cell line. Phalloidin staining for ARAP3 knockdown 44As3 cells (R3 and R5 cells) was performed (A). Wild-type ARAP3, which contained silent mutations in the microRNA target sequence, was stably introduced into R3 cells. Morphological changes were shown by phalloidin staining (Ba) and expression of ARAP3 was detected by western blotting (Bb). Formation of lamellipodia is indicated with yellow lines and filopodia is marked with yellow arrow heads.

changes (Carragher and Frame, 2004), we examined whether the expression of ARAP3 also affects the cell morphology of the gastric carcinoma cell line. Phalloidin staining showed that R3 and R5 cells formed filopodia instead of the lamellipodia observed in parental 44As3 cells (Figure 5A). Furthermore, introduction of wild-type ARAP3 that contained silent mutations in the target sequence of microRNA into R3 cells suppressed filopodia formation and recovered lamellipodia formation (Figure 5Ba). Expression of mutant ARAP3 was detected with western blotting (Figure 5Bb).

Differential roles of functional domains of ARAP3 in cell adhesion and cell invasion in vitro

As ARAP3 is a multimodular protein (Figure 6A), we investigated the structure–function relationships of ARAP3 domains to peritoneal dissemination. We established three 58As9 cells that expressed mutant ARAP3: (1) an Arf-GAP domain mutant (R532K), (2) a Rho-GAP domain mutant (R942L) and (3) a mutant that lacks both putative tyrosine phosphorylation sites (2YF, Y1403/1408F) (I *et al.*, 2004) (Figure 6A). The level of tyrosine phosphorylation of the ARAP3 2YF mutant was significantly reduced compared with R532K or R942L in 58As9 cells (Figure 6B). As expression levels of ARAP3 were associated with cell morphology in gastric cancer cells (Figure 5), we performed phalloidin staining for 58As9 cells overexpressing ARAP3 mutants. R532K mutant ARAP3 suppressed filopodia formation more strongly than R942L or 2YF mutants (Figure 6C). None of the ARAP3 mutants affected the growth of 58As9 cells (Supplemental Figure 2).

We also studied the effect of overexpression of each mutant ARAP3 on cell-ECM adhesion and invasion. Overexpression of the R532K mutant ARAP3 reduced the attachment of 58As9 cell lines to ECM proteins, but overexpression of the R942L and 2YF mutants did not have any effect (Figure 7A).

As overexpression of wild-type ARAP3 could inhibit the metastasis of 58As9 cells, we performed an *in vitro* migration and invasion assay with the ARAP3 mutant cells. The results of this assay were similar to the attachment assay. Specifically, overexpression of the R532K mutant inhibited cell migration and invasion, but the R942L and 2YF mutants did not have any effect (Figure 7B).

These results suggest that both Rho-GAP function and tyrosine phosphorylation of ARAP3 are necessary to suppress cell-ECM adhesion and invasion of gastric cancer cells. As ARAP3 can inhibit RhoA, which is required for cell invasion (Itoh *et al.*, 1999), we tested whether inhibition of RhoA signal by Y27632, one of the general inhibitors of Rho-associated coiled-coil kinase (ROCK), can also suppress the invasiveness of ARAP3 mutant expressing 58As9 cells. As expected, Y27632 could modestly suppress the invasiveness of the cells (Figure 7Bc).

Functional domains of ARAP3 critical for suppressing peritoneal dissemination in vivo

To investigate whether expression of mutant ARAP3 affects peritoneal dissemination *in vivo*, we injected the

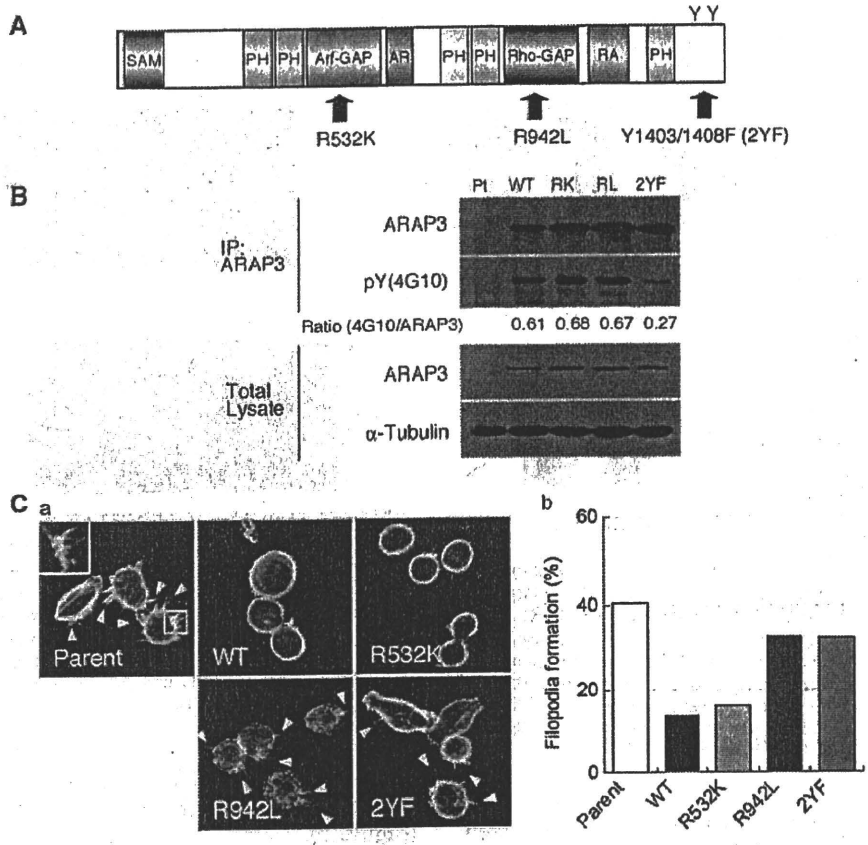

Figure 6 Expression of ARAP3 mutants. Mutations were introduced into the Arf-GAP (R532K) or Rho-GAP (R942L) domain, or into the two putative tyrosine phosphorylation sites (2YF) of ARAP3 (**A**). Expression and tyrosine phosphorylation profiles of 58As9 cells expressing mutant ARAP3 were verified by immunoprecipitation and immunoblotting. The relative tyrosine phosphorylation levels of ARAP3 (phosphorylated ARAP3/total ARAP3) were also calculated (**B**). Morphologies of cells expressing mutant ARAP3 are shown in (**C**). Phalloidin staining was performed on these cells. R532K mutant suppressed the filopodia formation that was observed in the parental cell line, but the R942L and 2YF mutants were not. Filopodia are indicated by white arrows. A highly magnified image of the area that is indicated by the white line is also shown in the image. Quantification of filopodia formation was performed by calculating the percentage of filopodia-positive cells (Cb). Over 100 cells were counted. SAM, sterile alpha motif; PH, pleckstrin homology domain; AR, ankyrin repeats; RA, Ras association domain (nearly conserved).

cells intraperitoneally into BALB/c nude mice (Figure 8). Parental 58As9 cells showed severe peritoneal dissemination with ascitic fluid as previously described (Yanagihara *et al.*, 2005). The R532K mutant suppressed production of ascitic fluid equally effectively, whereas the R942L and 2YF mutants were less effective (Figure 8A). Consistent with this result, expression of R532K, but not R942L and 2YF, suppressed the peritoneal dissemination of 58As9 cells, which was quantified by counting the number of mesentery nodules formed (Figure 8B). These results show that ARAP3 inhibits peritoneal dissemination *in vivo*, and that both the Rho-GAP domain and phosphotyrosine residues at the C-terminus are important for this function.

Discussion

This study showed that ARAP3 is expressed in normal fundic gland mucosa, but its expression is reduced in poorly differentiated carcinomas. ARAP3 inhibited not only cell-ECM attachment and cell invasion *in vitro* but also peritoneal dissemination of 58As9 cells *in vivo*. As adhesion to and invasion through the ECM are essential steps for peritoneal dissemination of scirrhous gastric carcinoma cells, it is hypothesized that ARAP3 suppresses peritoneal dissemination by regulating these processes enhanced in cancer cells.

We first identified ARAP3 while screening for phosphotyrosine proteins in mesentery nodules formed after inoculating nude mice with the 44As3 gastric carcinoma cell line. Unlike other phosphotyrosine proteins identified in this screening, such as FAK, CDCP1 and C9orf10/Ossa, ARAP3 was underexpressed in undifferentiated gastric cancers compared with normal fundic glands. Src pathways are implicated in cancer progression because SFK activity and expression and tyrosine phosphorylation of Src substrates are often elevated in advanced stages of cancer (Yeatman, 2004). Although ARAP3 is a Src substrate, our results showed that tyrosine phosphorylation of ARAP3 conferred

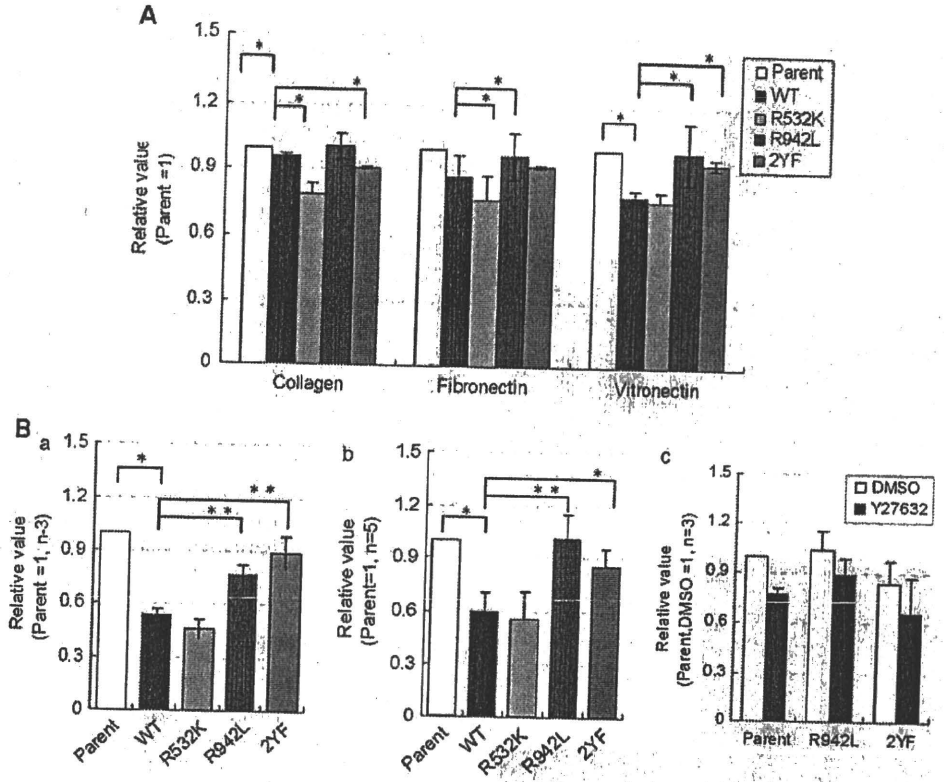

Figure 7 Effects of overexpression of ARAP3 mutants in 58As9 cell lines. Adhesiveness and invasiveness were examined by a cell attachment assay (**A**) and a cell migration and invasion assay (**Ba** and **Bb**, respectively). Overexpressed R942L and 2YF mutants did not rapidly adhere to ECM proteins or suppress cell migration and invasion. The Rho-associated coiled-coil kinase (ROCK) inhibitor Y27632 suppressed the invasiveness of 58As9 cells expressing R942L or 2YF ARAP3 (**Bc**). ARAP3 may suppress the invasiveness of 58As9 cells *in vitro* by inhibiting RhoA activity (*$P<0.05$ **$P<0.01$).

a tumor suppressive activity. As a result, SFKs may phosphorylate not only oncogenic proteins but also tumor suppressor proteins such as ARAP3.

The ability of ARAP3 to suppress peritoneal dissemination was blocked by a mutation in the Rho-GAP domain, suggesting that this function is mediated by regulation of the Rho family small GTPases. In addition, loss of the C-terminal tyrosine phosphorylation sites of ARAP3 also reduced this suppressive function of ARAP3. However, it is not clear whether Rho-GAP activity and tyrosine phosphorylation of ARAP3 regulate the peritoneal dissemination using an overlapping mechanism or a signal pathway, as no information is available on the phosphotyrosine-mediated signaling of ARAP3. Although we could not detect any change in the activities of Rho family small GTPases in total cell lysate (data not shown), we cannot rule out the possibility that the activation of Rho occurs at the cell surface, because ARAP3 can localize and function there (Krugmann *et al.*, 2002), and its expression actually affected their cytoskeletal reorganization.

Rho family small GTPases are involved in a wide range of cellular processes, such as cell morphology, adhesion and motility. For example, activation of RhoA promotes the stabilization of focal contacts, which are important in the integrin-dependent cell-ECM attachment and cell invasion (Huveneers and Danen, 2009). Filopodia formation is necessary for cell migration and contact sites formation. In neuronal cells, RhoA activity is necessary for the formation of filopodial protrusion induced by RhoA/ROCK signaling (Chen *et al.*, 2006; Kim *et al.*, 2010). Furthermore, activation of mammalian diaphanous-related formin (mDia), which is known as an effector of RhoA, localizes at the filopodia, promotes actin filament assembly and contributes to filopodia formation (Faix and Grosse, 2006; Carramusa *et al.*, 2007; Sarmiento *et al.*, 2008). Therefore, ARAP3 may suppress the cell adhesion, migration and invasion of cancer cells by inhibiting RhoA signaling through its Rho-GAP domain.

ARAP3 is a multimodular protein that can bind to several molecules such as PI(3,4,5)P3 and Src homology 2 domain containing inositol 5-phosphatase 2 (SHIP2) *in vitro*, possibly through its sterile alpha motif domain (Krugmann *et al.*, 2002; Raaijmakers *et al.*, 2007). Our data revealed the essential role of the phosphotyrosine-containing region of ARAP3 for the first time. It might be required to identify molecules that bind to the C-terminal region of ARAP3 in a tyrosine phosphorylation-dependent manner. Further study is needed to determine